Apical Plasma Membrane Proteins and Endolyn-78 Travel through a Subapical Compartment in Polarized WIF-B Hepatocytes

Gudrun Ihrke,* Greg V. Martin,* Michael R. Shanks,* Michael Schrader,‡ Trina A. Schroer,‡ and Ann L. Hubbard*

*Department of Cell Biology and Anatomy, The Johns Hopkins School of Medicine, Baltimore, Maryland 21205; and ‡Department of Biology, Johns Hopkins University, Baltimore, Maryland 21218

Abstract. We studied basolateral-to-apical transcytosis of three classes of apical plasma membrane (PM) proteins in polarized hepatic WIF-B cells and then compared it to the endocytic trafficking of basolaterally recycling membrane proteins. We used antibodies to label the basolateral cohort of proteins at the surface of living cells and then followed their trafficking at 37°C by indirect immunofluorescence. The apical PM proteins aminopeptidase N, 5′nucleotidase, and the polymeric IgA receptor were efficiently transcytosed. Delivery to the apical PM was confirmed by microinjection of secondary antibodies into the bile canalicular-like space and by EM studies. Before acquiring their apical steady-state distribution, the trafficked antibodies accumulated in a subapical compartment, which had a unique tubulovesicular appearance by EM. In contrast, antibodies to the receptors for asialoglycoproteins and mannose-6-phosphate or to the lysosomal membrane protein, lgp120, distributed to endosomes or lysosomes, respectively, without accumulating in the subapical area. However, the route taken by the endosomal/lysosomal protein endolyn-78 partially resembled the transcytotic pathway, since anti–endolyn-78 antibodies were found in a subapical compartment before delivery to lysosomes. Our results suggest that in WIF-B cells, transcytotic molecules pass through a subapical compartment that functions as a second sorting site for a subset of basolaterally endocytosed membrane proteins reaching this compartment.

Polarity is a fundamental characteristic of most eukaryotic cells, either as a transient phenomenon (e.g., in a moving fibroblast) or a permanent feature (e.g., of an epithelial layer) (Drubin and Nelson, 1996). In epithelial cells, polarity is evident at many levels. At the cell surface, the basolateral and apical membrane domains face different environments (internal and external, respectively) and each membrane contains a distinct set of proteins and lipids (Simons and Fuller, 1985). Acquisition of the fully polarized epithelial phenotype requires assembly of tight and adhering junctions, which serve as barriers separating the apical and basolateral surfaces, and the selective delivery of plasma membrane (PM)[1] molecules and/or their retention at each surface (Rodriguez-Boulan and Powell, 1992; Simons et al., 1992; Wollner and Nelson, 1992).

There is great variety among epithelial cells in the way specific PM proteins reach the same or different destinations. For example, kidney-derived MDCK cells sort most apical and basolateral membrane components in the TGN and then export this cargo directly to the "correct" surface (Matter and Mellman, 1994), although a variant line was recently found that delivers Na^+,K^+-ATPase to all PM domains randomly and then achieves a predominant basolateral distribution by selective retention (Hammerton et al., 1991; Mays et al., 1995). In other epithelial cells, apical PM proteins are first transported to the basolateral surface and then subsequently transcytosed to the apical domain, with sorting occurring in the endocytic pathway. The extent to which this more circuitous or "indirect" pathway to the apical surface is used depends on the specific protein and cell type (Rodriguez-Boulan and Zurzolo, 1993; Matter and Mellman, 1994). For delivery of apical membrane proteins, hepatocytes in vivo appear to use the indirect pathway exclusively (Bartles et al., 1987; Schell et al., 1992; Maurice et al., 1994), whereas cultured HepG2 cells re-

G. Ihrke's present address is Department of Clinical Biochemistry, University of Cambridge, Addenbrooke's Hospital, Cambridge CB2 2QR, UK.

Address all correspondence to Ann L. Hubbard, Department of Cell Biology and Anatomy, The Johns Hopkins School of Medicine, 725 North Wolfe Street, Baltimore, MD 21205. Tel.: (410) 955-2333. Fax: (410) 995-1013. E-mail: alh@welchlink.welch.jhu.edu

1. *Abbreviations used in this paper*: 5′NT, 5′-nucleotidase; APN, aminopeptidase N; ASGP-R, asialoglycoprotein receptor; BC, canalicular-like space(s); DPPIV, dipeptidyl peptidase IV; GPI, glycosyl phosphatidyl inositol; HSFM, Hepes-buffered serum-free medium; IMF, indirect immunofluorescence; M6P-R, mannose-6-phosphate receptor; pIgA-R, polymeric IgA receptor; pAb, polyclonal antibody; PM, plasma membrane; r.t., room temperature; SAC, subapical compartment; Tf, transferrin; Tf-R, transferrin receptor.

portedly deliver selected membrane lipids directly from the TGN to the apical PM (Zaal et al., 1994).

The structural information directing membrane proteins through the transcytotic pathway has been elucidated only for the polymeric IgA receptor (pIgA-R). It is a sacrificial receptor whose 103-amino acid cytoplasmic tail contains multiple signals that direct the protein through the secretory pathway and into the transcytotic branch of the endocytic system. pIgA-R's final destination is the apical membrane where an 80-kD proteolytic fragment of the receptor's ectodomain is released into the apical milieu. An important difference between the pIgA-R and resident apical PM proteins studied so far is that the latter usually have short cytoplasmic tails with no apparent sorting signal (e.g., aminopeptiase N [APN] and dipeptidyl peptidase IV [DPPIV]), or are glycosyl phosphatidyl inositol (GPI)-anchored (e.g., 5′-nucleotidase [5′NT]). Positive sorting information is present elsewhere in these proteins, e.g., the glycolipid anchor of GPI-proteins (Lisanti and Rodriguez-Boulan, 1990) and the large ectodomains of APN and DPPIV (Vogel et al., 1992, 1995; Weisz et al., 1992), but finer resolution of such global signals has not yet been attained.

Many studies have described the membrane compartments involved in the basolateral-to-apical transcytosis of soluble and/or membrane-bound cargo (e.g., Bomsel et al., 1989; Brändli et al., 1990; Hayakawa et al., 1990; van Deurs et al., 1990; van Genderen and van Meer, 1995). Although it is now clear that multiple compartments participate, the existence of stations or carriers that are unique to the transcytotic pathway is still an open question (e.g., Barroso and Sztul, 1994, versus Apodaca et al., 1994), as are the number and location(s) of the sorting site(s) for transcytotic cargo versus cargo destined for the recycling or lysosomal branches of the endocytic system (for reviews see Courtoy, 1993; Sandoval and Bakke, 1994; Gruenberg and Maxfield, 1995; Mostov and Cardone, 1995). The remarkable plasticity of the endocytic system as well as the possibility of real differences in the transport of soluble and membrane cargo may explain some of the apparent paradoxes. Early immuno-EM studies reported that in hepatocytes in vivo, the pIgA-R shares clathrin-coated entry sites with receptors that recycle between the PM and endosomal compartments (asialoglycoprotein receptor [ASGP-R] and mannose-6-phosphate receptor [M6P-R]), but is then segregated from them at the level of peripheral endosomes (called compartment for uncoupling of receptors and ligands) (Geuze et al., 1984). In contrast, the entry site(s) for resident apical proteins transiently present at the basolateral surface is still unknown. However, in liver in situ, newly synthesized DPPIV colocalizes with transcytosing pIgA-R in subapical tubulovesicular structures, suggesting that, at least in these cells, the last steps of transcytosis are common (Barr and Hubbard, 1993). Moreover, transcytotic membranes can be isolated that contain pIgA-R and newly synthesized DPPIV (Barr et al., 1995). Nevertheless, the extent to which different membrane protein classes with a common destination share a common pathway is still unclear.

The newly developed WIF-B cell line is an ideal in vitro model for studying PM protein trafficking in polarized hepatocytes (Ihrke et al., 1993; Shanks et al., 1994). WIF-B cells grow in monolayers and acquire a polarized phenotype reminiscent of hepatocytes in vivo; that is, neighboring cells form bile canalicular-like spaces (BC). Each BC is completely sequestered from the surrounding medium as well as the substratum and apical PM proteins are highly concentrated in the BC membrane. Tight junctions prevent mixing of apical and basolateral PM proteins and block diffusion of large molecules such as antibodies from the culture medium into the BC (Ihrke et al., 1993).

As a first step toward understanding the transcytotic pathway(s) in WIF-B cells and ultimately in liver, we define here the intracellular trafficking pathways taken by three different classes of membrane proteins that pass through the basolateral membrane: (*a*) apical PM proteins and pIgA-R; (*b*) basolaterally recycling receptors; and (*c*) proteins of the endosomal/lysosomal pathway that cycle through the PM. These proteins were tracked in living WIF-B cells by labeling with specific antibodies at the basolateral surface and determining the distributions of the antigen–antibody complexes at later times. Antibodies to a variety of apical PM proteins and the pIgA-R were specifically and efficiently transcytosed from the basolateral to the apical domain; all passed through a prominent subapical compartment before fusion with the apical PM. In contrast, antibodies to cycling membrane proteins, such as the ASGP-R, transferrin receptor (Tf-R), and M6P-R, and the lysosomal membrane protein lgp120, did not appear to pass through the subapical compartment, but rather were directly transported to the intracellular compartments that contained the highest concentrations of their antigens at steady state. However, antibodies to endolyn-78, another endosomal/lysosomal membrane protein (Croze et al., 1989), appeared transiently in the apical region of the cells before accumulating in lysosomes. Thus, the trafficking of endolyn-78 resembled to some degree the transcytotic route of apical PM proteins and pIgA-R.

Our observations verify that transcytosis is a pathway for the delivery of apical PM proteins to the apical surface in WIF-B cells, as is seen in hepatocytes in vivo. Our findings suggest that two successive sorting compartments operate in WIF-B cells. Basolaterally endocytosed proteins pass first through peripheral endosomes, the compartment from which most ASGP-R and transferrin receptor (Tf-R) molecules recycle; from there lysosomal proteins such as lgp120 are directed towards lysosomes whereas transcytotic molecules are sorted out for transport to the apical pole. However, segregation of apical residents from at least one endosomal/lysosomal marker, endolyn-78, appears to occur after these proteins are delivered to an endomembrane compartment in the subapical region.[2]

Materials and Methods

Medium nutrient mixture Ham's F-12 (Cassio modified; Coon and Weiss, 1969; Cassio et al., 1991) was obtained from Gibco Laboratories (Grand

2. Portions of this work have been presented in abstract form: Ihrke, G., K. Finnegan, and A.L. Hubbard. 1993. Transcytosis of apical plasma membrane proteins in the hepatoma-derived WIF-B cell line. *Mol. Biol. Cell.* 4:97*a*; Ihrke, G., and A.L. Hubbard. 1995. Trafficking of plasma membrane proteins in polarized WIF-B hepatocytes. *Eur. J. Cell Biol.* (Suppl.):214; Shanks, M.R., H. Fujita, and A.L. Hubbard. 1996. Microinjection of antibodies to detect delivery of membrane proteins at the apical surface in WIF-B cells. *Mol. Biol. Cell.* 7:517*a.*

Island, NY); FCS was supplied from Hyclone (Logan, UT); fluorescently or gold-labeled secondary antibodies were from Jackson ImmunoResearch Laboratories, Inc. (West Grove, PA); carrier-free Na^{125}iodine was from Amersham Corp. (Arlington Heights, IL) as were bisfunctional reactive dyes that were used to prepare Cy3- and fluorescein-labeled immunoglobulins and transferrin (Tf); amine-activated HRP was obtained from Pierce Chemical Co. (Rockford, IL). All other chemicals were from Sigma Chemical Co. (St. Louis, MO).

Primary Antibodies

The mouse mAbs to HA4, HA321, and pIgA-R (SC455) have been described (Hubbard et al., 1985; Scott and Hubbard, 1992), as have the rabbit polyclonal antibodies (pAbs) to ASGP-R, DPPIV, CE9, and pIgA-R (Bartles et al., 1985*a*,*b*; Hoppe et al., 1985). Rabbit pAb JH 1637 to APN was prepared by Covance (Denver, PA) using affinity-purified antigen from rat intestine. Mouse mAbs 501 and 502 were generated by a passive–active immunization of mice (Zhu and Pauli, 1991) to a carrier vesicle fraction depleted of PM and Golgi proteins (Ihrke, G., V. Barr, and A. Hubbard, manuscript in preparation). Mouse mAb 5N-H3 to 5′NT and rabbit pAb 580 to lgp110 were provided by P. Luzio (University of Cambridge, Cambridge, UK) (Bailyes et al., 1984; Reaves et al., 1996). Mouse mAb GM10 to lgp120 was supplied by K. Siddle and J. Hutton (both from University of Cambridge) (Grimaldi et al., 1987). Three different rabbit pAbs to rat lgp120 were used: pAb A3 from W.A. Dunn (University of Florida, Gainesville, FL) (Dunn, 1990) used for all steady-state labelings, anti-LGP107 from K. Kato, Y. Tanaka, and M. Himeno (all from Kyushu University, Fukuoka, Japan) (Furuno et al., 1989), and a third pAb (to lgp120 from NRK cells) from I. Mellman (Yale University, New Haven, CT) (Lewis et al., 1985). Rabbit pAb 3637 to M6P-R was provided by P. Nissley (National Institutes of Health, Bethesda, MD) (Kiess et al., 1987), and rabbit pAb JH 1481 to TGN 38 by R.E. Mains (Johns Hopkins University, Baltimore, MD) (Milgram et al., 1996). A mouse mAb to mannosidase II was purchased from Berkeley Antibody Company (Richmond, CA).

Cell Culture

WIF-B cells were cultured in a humidified 7% CO_2/93% air incubator at 37°C as described elsewhere (Shanks et al., 1994). Briefly, cells were grown in modified Ham's F12 medium supplemented with HAT (10 mM hypoxanthine, 0.04 mM aminopterin, 1.6 mM thymidine) and 5% FCS. Cells were routinely passaged on 100-mm plastic dishes (Falcon Plastic, Cockeysville, MD) at 2–2.5 $\times$ 10^5 cells/dish. For experiments, cells were plated onto glass coverslips at 1–2 $\times$ 10^6 cells/dish, using 100-mm dishes containing four UV-sterilized 22-mm^2 coverslips. 2 d after plating, each coverslip was transferred to a separate 60-mm dish and then fed with 5 ml of medium; thereafter, the cells were fed every 2 or 3 d. As necessary during the last 2–4 d of culture, cellular debris was removed by rinsing with PBS containing 0.9 mM $CaCl_2$, 0.52 mM $MgCl_2$, and 0.16 mM $MgSO_4$ (PBS^{2+}) before feeding every 1 or 2 d. For most experiments, cultures that had reached their maximal density and polarity, i.e., 9–12 d after sowing, were used. In Tf uptake experiments, 6–8 d-old cultures (60–70% confluency) were used; these cells already exhibited significant polarization ($\geq$50%).

Fluorescence Experiments

IMF on Fixed Cells. Cells on coverslips were fixed in 4% paraformaldehyde/PBS^{2+} for 1 min at 0°C, permeabilized in methanol for 10 min at 0°C, and then rehydrated in PBS (as described with minor modifications; Mevel-Ninio and Weiss, 1981). After blocking in 1% BSA/PBS, cells were incubated with primary antibodies at the following dilutions in 1% BSA/PBS: antisera to M6P-R (1:100) and to lgp120 (1:200); affinity-purified pAb to ASGP-R, and IgG prepared from ascites (mAb 501) were used at 10 μg/ml. After washes in PBS, cells were incubated with anti–mouse or anti–rabbit secondary antibodies (developed in goat or donkey, minimal cross reaction to other species) coupled to FITC (10 μg/ml), Texas red ($F[ab]_2$-fragments, 10 μg/ml), Cy3 (2–5 μg/ml), or Cy5 (5–10 μg/ml), washed again, and then mounted in 50% glycerol/PBS containing 2–3 mg/ml *p*-phenylenediamine. In double-labeling experiments, the cells were incubated with either both primary or both secondary antibodies at the same time. Photographs were taken on an epifluorescence microscope (model Axioplan; Carl Zeiss, Inc., Thornwood, NY) equipped with a 100× Zeiss objective. Confocal images representing 0.85–1.0-μm optical sections were collected with a Zeiss LSM410 microscope using a 100× Zeiss objective. The images shown in Fig. 7, *C* and *C′* were generated on a confocal imaging system (model MRC 600; Bio-Rad Laboratories, Hercules, CA) with a 63× Zeiss objective. Single images were processed such that the available range of gray levels were used without saturation using Adobe Photoshop (Adobe Systems, San Jose, CA) or Metamorph software (Universal Imaging, Woods Hole, MA).

Labeling of Living Cells with Antibodies. Cells on coverslips were washed twice with 2 ml of Hepes-buffered serum-free medium (HSFM), cooled to 4°C over ~5 min, and then labeled with one or two primary antibodies in 0.2% BSA/HSFM for 15 or 30 min in an ice/water bath (surface label). The following antibody concentrations were used: anti-5′NT mAb (10–100 μg/ml); anti–endolyn-78 mAb 501 (400 μg/ml); affinity-purified pAb to CE9 (20 μg/ml) and to ASGP-R (12.5 μg/ml); IgG fractions of antisera to APN (104 μg/ml) and to pIgA-R (128 μg/ml); the polyclonal antisera to APN and pIgA-R (used in Fig. 1) were diluted 1:100 and 1:200, respectively. After surface labeling, cells were washed once with 2 ml HSFM, five times for 2 min with 1 ml 0.2% albumin/HSFM, and then again with 2 ml of HSFM. Cells were subsequently incubated at 37°C in normal culture medium (7% CO_2) for different lengths of time, washed two times briefly with PBS^{2+}, and then fixed and incubated with fluorescently labeled secondary antibody as described for indirect immunofluorescence (IMF). For the trafficking of anti–endolyn-78 mAb, the 37°C-incubation was done in the presence of 42 μM leupeptin to minimize degradation of antibody in lysosomes. Control cells (no warming) were fixed directly after the primary antibody incubation and washes. Fixed cells were incubated with secondary fluorescently labeled antibodies (10–20 μg/ml) to detect trafficked antibodies and then further treated as described for IMF. In some cases, fixed cells were incubated with another primary antibody to detect the steady-state distribution of a second antigen before incubation with secondary antibodies. Confocal microscopy was done as described above.

In constant uptake experiments at 37°C, cells were washed once with warm complete culture medium containing 20 mM Hepes and then incubated with antibody in the same medium at 37°C in the presence or absence of 42 μM leupeptin (with qualitatively similar results). In these experiments, mAb 501 (to endolyn-78) was used at 20 μg/ml, GM10 ascites (to lgp120) at 1:25, and anti-APN total IgG from antiserum at 8 μg/ml. Washes and fixation were done at 0°C as before.

Fab fragments were prepared by papain digestion as described (Porter, 1959) using an Immobilized Papain Kit from Pierce Chemical Co. The electrophoretic profiles of the papain cleavage products were analyzed by 10% SDS-PAGE and Coomassie blue staining. There was no intact IgG nor $F(ab)_2$ detected in the Fab fraction under reducing or nonreducing conditions (data not shown). Parallel sets of cells on coverslips were incubated with 10–40 μg/ml (anti-5′NT) or 120 μg/ml (anti-APN) Fab, or similar concentrations of the corresponding IgGs under identical conditions, and then processed as for IMF.

Labeling of Living Cells with Tf. Human Tf was saturated with iron (Yamashiro et al., 1984) and then subsequently conjugated to Cy3 according to the manufacturer's instructions (Amersham Corp.). All steps of the cell labeling procedure, except permeabilization, were performed at 37°C and/or with buffers warmed to 37°C. Cells were preincubated for 3 h in serum-free medium, washed once with 0.2% ovalbumin/HSFM, and then incubated for 30 min with 30 μg/ml Tf-Cy3 in 0.2% ovalbumin/HSFM. At the end of the incubation, cells were washed twice with 0.2% ovalbumin/HSFM, once with HSFM, and then once briefly with PBS^{2+}. The cells were then fixed in 4% paraformaldehyde/100 mM cacodylate buffer containing 3 mM KCl, 3 mM $MgCl_2$, and 0.9 mM $CaCl_2$ for 15 min, permeabilized with methanol on ice for 10 min, and then rehydrated in PBS. In double-labeling experiments, cells were further treated as described for IMF. We observed the same labeling pattern and comparable staining intensity with Tf-Cy3 when, before incubation with Tf-Cy3, cells were incubated in 0.2% ovalbumin/HSFM for 15 min with four changes of the medium instead of a prolonged period in serum-free medium. Specificity of Tf-Cy3 binding was confirmed by incubation of cells on parallel dishes in the presence of a 100-fold excess of unconjugated, iron-saturated Tf, a condition that abolished binding of conjugated ligand. Moreover, almost all fluorescence was lost within 30 min when labeled cells were incubated further in the presence of 1 mg/ml of unlabeled ligand and 10 mM of deferoxamine mesylate.

Microinjection of Fixed WIF-B Cells. Cells were washed in HSFM, cooled to 4°C over 3 min, and then incubated with one of the following primary antibodies in HSFM for 20 min at 4°C: anti-APN and anti-pIgA-R (antiserum 1:100), anti-HA4 mAb (150–300 μg/ml), anti–endolyn-78 (mAbs 501 or 502; 300–400 μg/ml), and fluorescein-conjugated anti-5′NT mAb (20 μg/ml). Cells were then washed three times for 3 min in HSFM at 4°C, reincu-

bated in normal culture medium at 37°C (7% CO_2) for various times, subsequently fixed in 4% paraformaldehyde/PBS for 30 min at room temperature (r.t.), and then finally washed in PBS. BC of WIF-B cells immersed in PBS (r.t.) were microinjected either with 1 mg/ml Cy5-conjugated secondary antibody (donkey anti–rabbit IgG or donkey anti–mouse IgG) together with 0.2 mg/ml fluorescein-conjugated anti-5′NT as microinjection marker or, in the case of fluorescein-conjugated anti-5′NT as trafficked antibody, with 1 mg/ml Cy5-conjugated donkey anti–mouse IgG together with 40 mg/ml TRITC-conjugated WGA; all antibodies were diluted in PBS. Each BC was microinjected for 0.5 s at 250 hPa pressure using an Eppendorf Transjector 5246 and Micromanipulator 5171 (both from Eppendorf Scientific, Inc., Hamburg, Germany) attached to a Zeiss Axiovert 100 microscope equipped with a 32× objective. Between 20–60 microinjections were performed on each coverslip. After microinjection, cells were fixed a second time in 4% paraformaldehyde/PBS (for 10 min at r.t.). To visualize the total population of trafficked primary antibodies that were not directly conjugated to a fluorophore, cells were permeabilized in methanol for 5 min at 4°C after the second fixation, rehydrated in PBS for 15 min at r.t., and then incubated with Cy3-conjugated secondary antibody (5 μg/ml). Mounted samples (refer to IMF) were analyzed using a laser scanning confocal microscope (model LSM410; Carl Zeiss, Inc.) with a 100× Zeiss objective collecting images from 0.9-μm optical sections. Between 50–100% of all microinjected BC could be found after these manipulations. All digitized images were processed and then analyzed using Adobe Photoshop 3.5 (Adobe Systems Inc.).

A set of four corresponding images, one phase contrast and three colors of fluorescence, was used to quantify the delivery of the different markers to the subapical region and the BC PM (see Fig. 4): (*a*) phase contrast (to locate all BC in a field); (*b*) microinjected marker (to identify the microinjected BC); (*c*) microinjected secondary antibody (to identify the positively labeled BC); and (*d*) trafficked primary antibody (to identify positively labeled subapical regions). In the last case (*d*), cells were scored positive if they exhibited a halo or crescent labeling pattern that extended ~1.5 μm from the BC membrane but was distinct from *c*. In addition to Fig. 4, typical examples of subapical regions can be seen in Fig. 6 (*A–A″*, *B–B″*, and *D–D″*), Fig. 8 (*C–C″* and *D–D″*), and Fig. 9 (*A*, *A′*, and *B′*).

Electron Microscopy

Labeling of Ultrathin Cryosections. Cells were rinsed in Hank's buffer (90.3 mM NaCl, 4.2 mM KCl, 1 mM Na_2HPO_4, 0.6 mM KH_2PO_4, 1.2 mM $NaHCO_3$, 0.6 mM dextrose), pH 7.4, fixed (3% paraformaldehyde, 0.05% glutaraldehyde, 3% PVP-40, 70 mM NaN_3 in Hank's buffer; Roth et al., 1985) at 37°C for 10 min on the dish, removed by scraping, and then pelleted for 10 min at maximal speed in a microfuge (model Shelton Scientific VSMC-13; Vangard International, Inc., Neptune, NJ). Cell pellets were incubated in the same fixative for another 40 min at 37°C, cut into 1–2 mm^2 blocks, rinsed briefly in fixation buffer (without fixative), and then infiltrated with a carbonate-phosphate buffer containing 50% polyvinylpyrrolidone (mol wt 10,000) and 2.3 M sucrose (Tokuyasu, 1989) for 2 h at r.t. before being frozen in liquid nitrogen. The specimens were sectioned and labeled as described elsewhere (Tokuyasu, 1989) with some modifications. Briefly, silver to gold ultrathin cryosections were cut with glass knives at −110°C, collected with a drop of 2.3 M sucrose, 0.75% gelatin in 0.1 M sodium phosphate buffer, pH 7.2, and then placed on carbon formvar-coated nickel grids after thawing. The sections were rinsed five times for 5 min in 1% FCS/PBS, blocked in 10% FCS/PBS for 15 min, and then incubated for 1 h with anti-5′NT mAb (20 mg/ml). Unbound antibody was removed by eight brief rinses followed by three 10-min rinses with 10% FCS/PBS. Sections were incubated with colloidal gold-conjugated donkey anti–mouse or anti–rabbit antibody in 10% FCS/PBS (OD_{520} = 0.05 for gold probe) for 60 min and then washed as before. The sections were further rinsed twice for 2 min in PBS, fixed with 2% glutaraldehyde in PBS for 10 min, and then rinsed again, twice for 2 min in PBS and once briefly in dH_2O. This was followed by incubation in 2% OsO_4 (aq) for 20 min, two 2-min rinses with dH_2O, and then further staining with 2% uranyl acetate (aq) for 45 min. Final embedding/contrasting of the sections was accomplished by incubating the sections in 2.5% polyvinyl alcohol (mol wt 10,000) for 2 min followed by 3 min in 2.5% polyvinyl alcohol containing 0.0015–0.002% lead citrate. The sections were observed and photographed with a Zeiss EM10 transmission electron microscope using an accelerating voltage of 80 kV.

Labeling of Living Cells with Gold-conjugated Antibody. Gold particles were prepared using the tannic acid/sodium citrate method as described (Slot and Geuze, 1985). Adsorption of IgG preparations of anti-5′NT mAb to the gold particles was carried out in 2 mM borax buffer, pH 9.5, using the minimal amount of IgG (0.75 mg/ml) needed to protect the gold particles from salt flocculation (Leunissen and De Mey, 1989). After the solution was adjusted to pH 8.2 and BSA added to a final concentration of 0.1%, the gold probe was concentrated and then sized on a sucrose gradient (Slot and Geuze, 1984). The final gold probe had an OD_{520} = 1.71 and a mean diameter of 3.6 ± 1.8 nm (n = 2403). Immunolabeling of 0.5-μm cryosections of WIF-B cells resulted in identical labeling patterns whether using the gold probe (diluted to an OD_{520} = 0.5) visualized by silver enhancement of the gold particles (Burry, 1995) or unconjugated mAb visualized by IMF. Gold-conjugated mAbs were dialyzed against HSFM, pH 7.5, and then supplemented with 1% BSA for binding and uptake by living cells. Since cells that were surface labeled using the standard conditions did not show sufficient signal for EM analysis, we incubated them with antibodies for 60 min at 37°C, washed as described for fluorescence experiments (0°C), and then chased for 3 h in normal culture medium at 37°C (7% CO_2). Control experiments using similar times of antibody uptake followed by processing for IMF showed that the overall trafficking pattern was not changed significantly under these conditions. Antibodies were still reaching the BC only by transcytosis (not paracellularly), since even after 60 min of constant antibody uptake, little to no labeling of the BC was seen if microtubules were depolymerized with nocodazole to block transcytosis. For EM, cells were fixed in 2% glutaraldehyde/0.1 M cacodylate buffer containing 3 mM KCl, $MgCl_2$, and $CaCl_2$ for 1 h at 37°C and then left overnight in fresh fixative at 4°C. All subsequent processing took place with the cells still attached to the coverslips and placed in Coplin jars. Cells were rinsed three times for 5 min with ice-cold 0.1 M cacodylate/7.5% sucrose, incubated for 1 h in ice-cold reduced OsO_4, and then followed by three 10-min rinses in cacodylate/sucrose at r.t. Specimens were dehydrated through a graded series of ethanol at r.t., and after three 5-min rinses in propylene oxide, they were incubated in a 1:2 mixture of Epon (Polysciences Inc., Warington, PA) in propylene oxide at 4°C on a rotator (Infiltron; Ted Pella Inc., Redding, CA). The specimens were brought to r.t., uncovered, and then left to rotate in a fume hood for 6 h to evaporate the propylene oxide. The infiltration resin was then exchanged for fresh Epon and the specimens were rotated overnight at r.t. and then followed by polymerization carried out at 60°C for 2 d. Coverslips were removed from the polymerized specimens by immersion in liquid nitrogen. Silver to gold ultrathin sections were stained with lead citrate for 5 min and then examined with a Zeiss EM10 transmission electron microscope operated at 60 kV. Sections were scanned at low magnification to positively identify BC. The apical membrane and subapical regions of BC that had gold probe at the apical plasma membrane were photographed at high magnification (20,000).

Labeling of Living Cells with IgG-HRP. IgG fractions (0.5–1 mg) of anti–endolyn-78 (mAb 501) or anti–APN pAb were conjugated to 1 mg amine-activated HRP, pH 7.2–7.6, according to the manufacturer's instructions and then the unbound HRP was removed by column chromatography (Freezyme Conjugate Purification Kit; Pierce Chemical Co.). The molar ratio of HRP to IgG in the resulting preparations was 0.5:1 to 1:1, respectively, as determined by HRP enzymatic activity (Hubbard and Cohn, 1972) and protein assays (BCA Protein Assay System; Pierce Chemical Co.). IgG–HRP conjugates were dialyzed against HSFM, pH 7.5, and then supplemented with 0.2% BSA for binding and uptake by living cells. Only those conjugates whose steady state and trafficking patterns exactly matched their native IgG were subsequently used in EM experiments. Cells on coverslips were incubated with 100 μg/ml of anti–APN–HRP or 30–70 μg/ml anti-endolyn-78–HRP for 30 or 45 min at 37°C. The continuous presence of HRP-conjugate for at least 30 min was necessary to adequately visualize them in the subapical compartment. Control cells were incubated either with no IgG or unconjugated IgG and then processed in parallel with the experimental sets. Cells were fixed as described above for anti–5′NT gold. After a 10-min fixation at r.t., cells were scraped off the coverslips, centrifuged at 10,000 *g* for 10 min in a microfuge, and then the supernate was removed and fresh fixative added to the pellet for an additional 30 min (total fixation time = 60 min). HRP activity was detected according to Venkatachalan and Fahimi (1969) using the modifications described previously (Wall et al., 1980; Hoppe et al., 1985). Cell pellets were dehydrated, embedded for electron microscopy, sectioned, and then examined unstained in the EM.

Quantitative analysis of the subcellular distribution of HRP-positive structures was performed on photographs at 15,500×. Unstained sections were systematically scanned at the EM and each complete BC encountered was photographed. A structure was defined as a BC if at least one apico-lateral junction was present and the apical membrane had microvilli. A minimum of four BC profiles were analyzed from each of three

independent experiments with two different anti–endolyn-78–HRP conjugates and from two independent experiments using two anti–APN–HRP preparations. The controls were sampled and then analyzed in an identical manner. The HRP-positive structures were categorized by shape and size into six different classes (see Fig. 10 for examples and Fig. 11 legend for definitions), and their distance was measured from the base of the nearest BC, in 0.5-μm increments up to 2 μm. More than 170 total HRP-positive structures were counted for each conjugate. The circumference of each BC, excluding microvilli, was measured using a piece of flexible tubing and expressed in millimeters.

Other Procedures

Metabolism of Internalized ^{125}I-Antibodies in Living Cells. IgG fractions of anti-5′NT mAb and anti–endolyn-78 (mAb 501) were iodinated with carrier-free Na^{125}I using modifications of the chloramine-T method (Greenwood et al., 1963), repurified by gel filtration on PD-10 columns (Pharmacia Biotech. Inc., Piscataway, NJ) in the presence of 1 mg/ml BSA, dialyzed against PBS overnight at 4°C, and then stored at −20°C in 20% ethylene glycol. Specific radioactivities were 1–2 × 10^7 cpm/μg. Cells grown on coverslips were washed as described above and then labeled with 1 μg/ml ^{125}I-anti–5′NT mAb for 15 min at 4°C or ^{125}I-mAb 501 for 30 min at 37°C. 200–1,000-fold excess unlabeled antibody was included in parallel sets to determine nonspecific binding/uptake. After antibody labeling, all cells were washed as described above and then incubated at 37°C in normal culture medium for different lengths of time. Cells exposed to 42 μM leupeptin were preincubated for 30 min at 37°C before addition of the antibody and were maintained in leupeptin through the subsequent steps. At the end of the incubation, the medium was collected and then the cells were solubilized in 25 mM Na(PO_4), 300 mM NaCl, 0.5% Triton X-100, 20 mM octylglucoside, pH 7.4, on ice for 30 min. Both medium and cells were precipitated in 10% TCA and centrifuged for 30 min at 4°C, after which the pellet and supernatant were separated and counted in a gamma counter (model 5500; Beckman Instrs., Inc., Palo Alto, CA). Nonspecific binding accounted for <10% and ~25% of the total anti-5′NT and anti–endolyn-78 initially bound, respectively, and was subtracted before calculations were made. TCA precipitable radioactivity found in the medium (a maximum of 30% of that initially bound) representing dissociated ^{125}I-IgG was not included in the degradation calculations. Degradation was expressed as percent of total activity [cpm_{sol} (M) + cpm_{sol} (C) + cpm_{ppt} (C)] that was TCA soluble [cpm_{sol} (M) + cpm_{sol} (C)].

Results

Antibodies to Apical PM Proteins Are Transcytosed across WIF-B Cells

The indirect pathway model of apical PM biogenesis predicts that newly synthesized apical PM proteins flux continuously through the basolateral membrane of WIF-B cells. As the intracellular itineraries of a variety of membrane proteins (e.g., lamp-1, Tf-R, and TGN38) have been successfully monitored in nonpolarized cells using antibody probes (Lippincott-Schwartz and Fambrough, 1986; Hopkins et al., 1990; Ladinsky and Howell, 1992), we chose a similar approach to visualize the trafficking behavior of basolaterally derived molecules on their way to the apical surface by light and electron microscopy. Among several apical markers tested (APN, 5′NT, DPPIV, and HA4), only 5′NT and APN could routinely be detected at low levels in the basolateral membrane by conventional IMF on fixed and permeabilized cells. However, we observed substantial basolateral labeling when living cells were incubated for 15–30 min at 0°C with antibodies to APN or 5′NT and then fixed and stained with fluorescently labeled secondary antibody (Fig. 1, *B* and *F*). Under similar conditions, DPPIV and HA4 could also be detected at the basolateral surface (data not shown). Importantly, although the vast majority of apical membrane proteins reside at the BC at steady state (Ihrke et al., 1993), the integrity of the tight junctions prohibited labeling of these molecules in living WIF-B cells. These results encouraged us to exploit the antibody trafficking approach to follow the dynamics of the basolateral population of apical PM proteins.

Since there is already extensive knowledge on the transcytosis of the pIgA-R in hepatocytes and other polarized cells in culture, we first compared the trafficking behaviors of the resident apical PM proteins with this receptor. Two differences distinguish the distributions of pIgA-R in hepatocytes in vivo and in WIF-B cells. First, within the population of WIF-B cells, the levels of expression of pIgA-R are more heterogeneous than for the other PM proteins. Second, its steady-state distribution indicates that the pIgA-R accumulates in the apical region of WIF-B cells, due to the fact that little pIgA-R is cleaved at the BC (our unpublished observation). This contrasts with the efficient cleavage of pIgA-R upon its arrival at the BC in vivo with subsequent release of the ectodomain into bile (Musil and Baenziger, 1988).

Despite their heterogeneous expression of pIgA-R, many WIF-B cells in the population contained adequate levels of protein for our trafficking studies. We simultaneously applied antibodies to pIgA-R and 5′NT and then determined their distributions over time (Fig. 1, *F–I′*). Fixation without warming revealed a patchy distribution of pIgA-R on the cell surface (Fig. 1, *F′*), as has been previously described for this and other endocytic receptors, and was observed when either a pAb (Fig. 1 *F′*) or a mAb (data not shown) to pIgA-R was used. This pattern differed from that of the four resident apical proteins that all displayed relatively homogeneous labeling at the basolateral surface with only a hint of fine punctate staining (as shown for APN and 5′NT in Fig. 1, *B* and *F*, respectively). When cells were warmed to 37°C before fixation, the staining pattern changed dramatically. For both the pIgA-R and apical proteins, the basolateral staining intensity decreased with a concomitant increase in staining in the apical region of the cells. Within a few minutes after warming the cells, most of the labeled pIgA-R was present in intracellular structures close to the basolateral surface (i.e., early endosomes), whereas 5′NT remained basolateral (data not shown). After 30–60 min, apical proteins and pIgA-R showed a subapical accumulation of fluorescence (Fig. 1, *C*, *G*, and *G′*, *arrows*). Although a subset of the subapical structures appeared to be positive for both the pIgA-R and 5′NT, the two labeling patterns were not completely coincident. At later time points (1–3 h), the antibodies to all three proteins became more homogeneously distributed along the BC membrane (Fig. 1, *D*, *I*, and *I′*). However, different from APN and 5′NT, some pIgA-R antibody could still be seen in intracellular compartments (Fig. 1 *I′*).

Trafficked antibodies reached their steady-state distribution with different kinetics. Interestingly, the order and approximate rates matched the behaviors of the respective apical PM proteins reaching the BC of hepatocytes in vivo, as measured by quantitative biochemical techniques (Bartles et al., 1987; Schell et al., 1992; Maurice et al., 1994). For example, antibodies to APN and pIgA-R reached maximal labeling in the BC region most quickly, after only 1–2 h, followed by anti-DPPIV (data not shown) and then

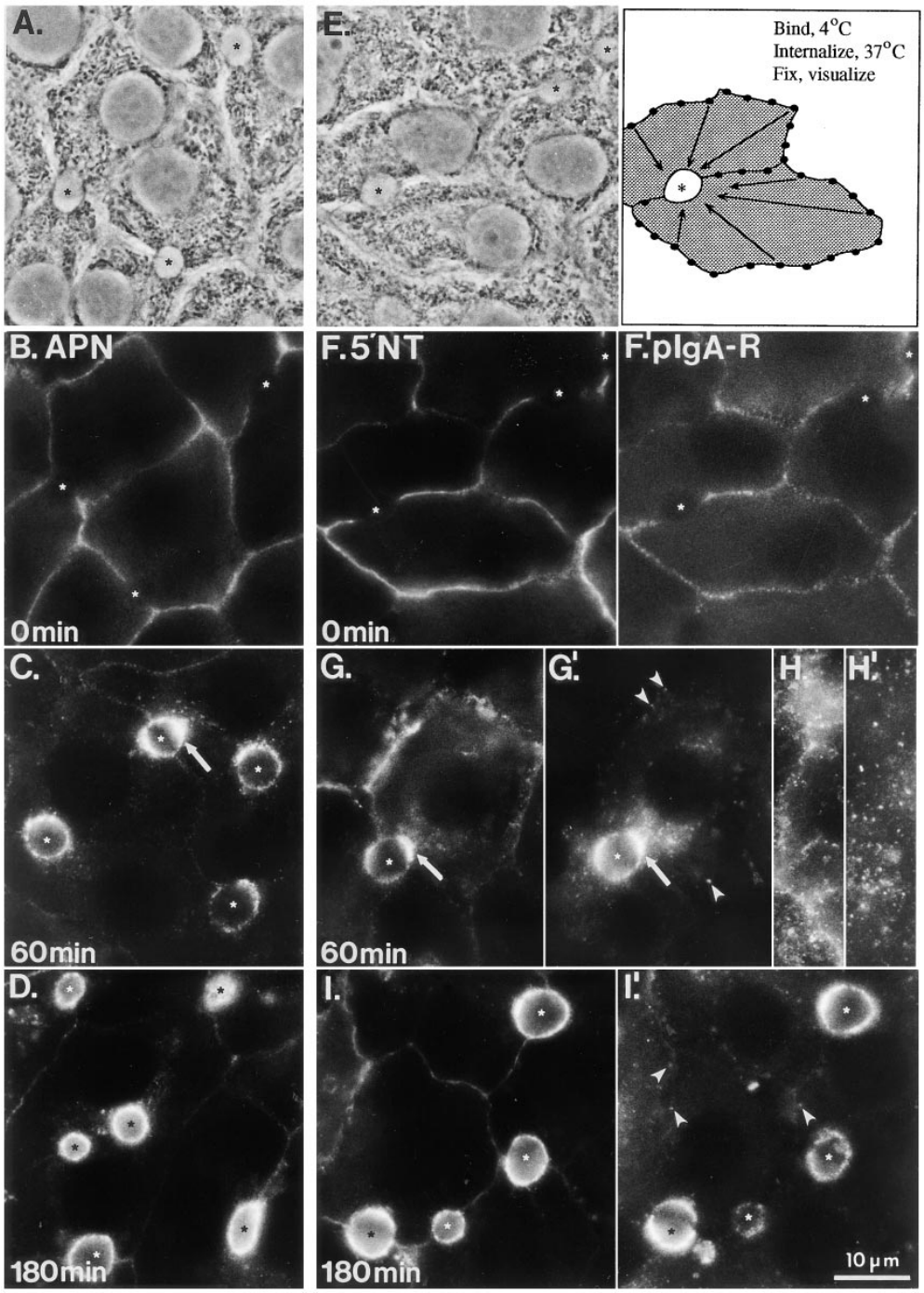

Figure 1. Basolateral-to-apical transcytosis of APN, 5′NT, and pIgA-R. Antibodies to the apical PM proteins APN (*B–D*) or 5′NT (*F–I*) and the pIgA-R (*F′–I′*) were bound to the basolateral surface of living WIF-B cells at 0°C (*middle* and *right panels* are double-labeled cells). The cells were washed and either fixed and permeabilized immediately (*B*, *F*, and *F′*) or incubated at 37°C for 60 (*C*, *G*, *G′*, *H*, and *H′*) or 180 min (*D*, *I*, and *I′*) before fixation and then permeabilization. Primary antibodies were visualized with FITC- (*APN* and *5′NT*) or Texas red-conjugated (*pIgA-R*) secondary antibodies. Pictures were generally focused on a plane near the middle of the cell where BC are seen best; a plane close to the substratum is shown in *H* and *H′* (*5′NT* and *pIgA-R*, respectively). *A* and *E* are the phase-contrast images of cells shown in *B* and *F*, respectively; *E′* is a schematic drawing depicting the transcytosis assay. Asterisks mark each BC, arrows (*C*, *G*, and *G′*) point to subapical accumulations of antigen–antibody complexes, and arrowheads (*G′* and *I′*) indicate peripheral pIgA-R–positive endosomes that were still detected at late chase times.

anti-5′NT, which reached its steady-state–like distribution after ~3 h. The kinetics of anti-HA4's approach to steady state were extremely slow, since significant HA4 labeling was still visible at the basolateral domain after 3 h, despite the fact that its steady-state distribution in WIF-B cells is overwhelmingly apical (Ihrke et al., 1993).

Transcytosis of Apical PM Proteins Is Selective and Specific

The validity of the transcytosis assay depended on the assumption that our antibodies were serving as faithful reporters of the membrane proteins to which they were bound, i.e., that the basal-to-apical transcytosis we observed was specific to a subset of membrane proteins and was not an antibody-induced phenomenon. Results of control experiments supported this assumption. First, since some divalent antibodies have been reported to cross-link their antigens and thus, alter the fate of that antigen (e.g., Tf-R; Weissman et al., 1986; Marsh et al., 1995), we compared the trafficking of both monoclonal and polyclonal intact IgGs to their corresponding monovalent Fab fragments. For the mAb, we chose to study 5′NT, reasoning that the GPI anchor would render this protein the most susceptible to cross-linking. For the pAb, we chose to study APN. Although the fluorescence signal of the Fab

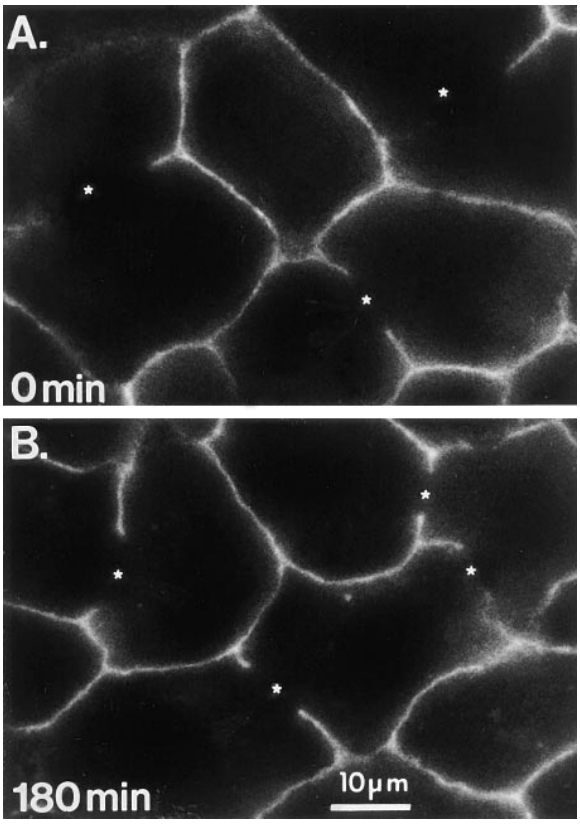

Figure 2. Antibodies to the basolateral PM protein CE9 are not transcytosed. Anti-CE9 pAb was bound to the basolateral surface of living WIF-B cells at 0°C. The cells were either fixed and permeabilized immediately (*A*) or incubated at 37°C for 180 min (*B*) before fixation and permeabilization. Primary antibodies were visualized by Cy3-conjugated secondary antibodies. *; BC.

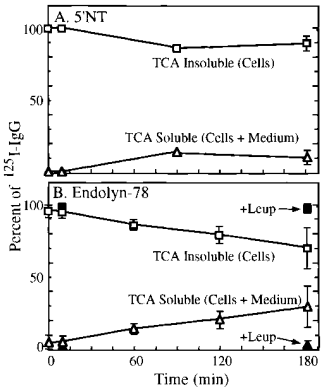

Figure 3. ^{125}I-labeled antibodies are stable during their intracellular trafficking. WIF-B cells were labeled with 1 μg/ml of ^{125}I-mAb to 5′NT (*A*; 0°C, 15 min) or to endolyn-78 (*B*; 37°C, 30 min). After incubation at 37°C for the indicated times, the medium was removed and then the cells were solubilized. Both medium and cell lysates were precipitated with TCA and the soluble (sol) and insoluble (ppt) radioactivities measured. Degradation (△) is expressed as percent of total activity that was TCA soluble; the TCA-insoluble radioactivity (□) represents cell-associated antibodies that are undegraded (refer to Materials and Methods). Degradation and percent precipitable activity were measured in the absence (△,□) or presence (▲,■) of leupeptin (*Leup*). Each time point represents the mean ± SD from at least three experiments done in triplicate.

fragments relative to the intact IgG was lower, we did not observe any significant difference in the trafficking pattern or the kinetics of the two probes (data not shown). Similar comparisons were not performed for the other antibodies, however, nonantibody endocytic tracers (Tf and alpha-2-macroglobulin) moved to identical-looking compartments in the same region of the cell, reinforcing the idea that antibodies to ASGP-R and M6P-R were trafficking to the appropriate compartment (data not shown). The second validation for the use of antibodies to track cognate proteins was our finding that antibodies to resident basolateral PM proteins, such as CE9 or HA321, were neither internalized nor transcytosed over a 3-h chase period (Fig. 2, *A* and *B*). This suggested that endocytosis and transport to the apical region was not simply induced by antibody binding. Furthermore, antibodies to apical PM proteins did not become trapped in an intracellular compartment (i.e., lysosomes) as might have been expected if they cross-linked antigen molecules or dissociated from the internalized antigen, causing them to be redirected to a degradative compartment (Anderson et al., 1982; Mellman and Plutner, 1984; von Figura et al., 1984). Indeed, when we purposely cross-linked membrane proteins by incubating the cells sequentially with primary (anti-5′NT) and an unlabeled secondary antibody at 4°C followed by an incubation at 37°C for ≤6 h, little, if any, antibody was delivered to the apical membrane. Instead, most label accumulated in large punctate structures or in clusters throughout the cells (data not shown). Finally, we measured the stability of the trafficked antibodies over the time course of the experiments using ^{125}I-labeled antibodies to 5′NT and endolyn-78 (see below). The data in Fig. 3 show that only ~10% of cell-associated 5′NT antibody was degraded over a 3-h period.

Transcytosed Apical PM Proteins Are Delivered to a Subapical Compartment before Reaching the BC Membrane

To distinguish between antibody-tagged apical PM proteins accumulating in an endomembrane compartment just beneath the surface and those actually being delivered to the BC membrane, we devised a method to directly visualize this latter pool of molecules. Unlike the apical PM surface in simple bipolar epithelial cells (e.g., MDCK cells), the apical PM domains of WIF-B cells are sequestered away from both the medium and substratum and are not easily accessed for experimental manipulation. To get around this problem and to specifically detect only antigen–antibody complexes that had been transcytosed to the apical surface, we microinjected fluorescent-labeled secondary antibodies into the BC spaces of paraformaldehyde-fixed cells after trafficking of primary antibodies. To identify those BC that had been microinjected, a general marker for the apical surface was injected in conjunction with the secondary antibody to the trafficked antigen–antibody complex. In the example shown in Fig. 4, anti-APN pAb was allowed to traffic for 0, 30, and 90 min at 37°C, the cells were fixed, and then the BC were microinjected with a mixture of secondary Cy5-conjugated anti-rabbit antibody (to tag APN) and FITC-conjugated anti-5′NT mAb (as general marker). To detect the entire population of trafficked anti-APN pAbs, including those remaining inside the cells, the cells were fixed a second time, permeabilized, and then incubated with secondary Cy3-conju-

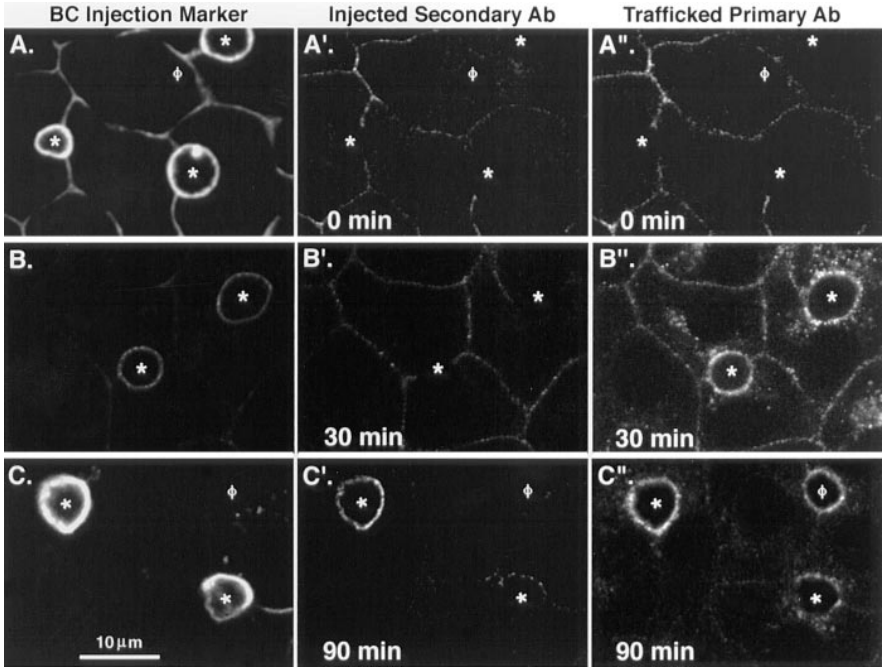

Figure 4. Arrival of transcytosed antibody–antigen complexes at the apical surface can be distinguished from delivery to the subapical region of WIF-B cells. Anti-APN pAb was bound to the surface of living WIF-B cells at 4°C and then allowed to traffic for 0 min (*A–A′′*), 30 min (*B–B′′*), or 90 min (*C–C′′*) at 37°C before fixation with paraformaldehyde. BC were microinjected with a mixture of fluorescein-conjugated anti-5′NT mAb as a marker for microinjected BC (*A–C*) and Cy5-conjugated secondary antibody to label transcytosed molecules (*A′–C′*). The entire population of trafficked APN–antibody complexes (i.e., surface and intracellular) was visualized by Cy3-conjugated secondary antibodies after a second round of fixation and permeabilization of the cells (*A–C′′*). Note that small amounts of both the microinjection marker (*A*) and injected secondary antibody (*A′* and *B′*) can be detected at the basolateral surface of all cells as a result of leakage from the needle during microinjection. *, microinjected BC; ϕ, noninjected BC.

gated anti-rabbit antibody. At 0 min after basolateral surface labeling, no trafficked antibody was detected at the membrane of microinjected BC, nor were trafficked molecules seen inside the cells (Fig. 4, *A′* and *A′′*, respectively; Fig. 5). After 30 min of warming, significant label could be seen in the apical region (Fig. 4 *B′′* Fig. 5), but the vast majority of these trafficked antibody–APN complexes were intracellular (i.e., subapical); in only a small subpopulation of BC could any trafficked antibody be detected at the apical surface (Fig. 4 *B′*; Fig. 5). However, after 90 min at 37°C, most BC were positive for transcytosed antibodies, with almost all of the label distributed between the apical surface and the region directly beneath (Fig. 4 *C′* and *C′′*; Fig. 5). The maximal number of BC labeled was achieved by 120 min, when the pattern of the microinjected secondary antibody (detecting only BC residents) could be superimposed upon that of the primary trafficked antibody.

These data suggested that structures in the subapical region were serving as intermediates between peripheral endosomes and the apical surface. To obtain a rough measure of the rate of delivery to the subapical region versus the BC surface, we quantified the staining in these two locations for three apical PM markers (APN, 5′NT, and HA4) and the pIgA-R at different chase times, analyzing ~200–550 microinjected BC for each protein (Fig. 5 *A*). We noted a clear precursor–product relationship between the appearance of complexes in the subapical region and the apical PM of microinjected cells. Since the subapical region and the BC were scored as being either positive or negative for staining rather than for relative intensity (amount), these kinetics reflect only the first detectable appearance of antibody in either compartment and not the rate of accumulation. Interestingly, most cells contained detectable antigen–antibody complexes in the subapical region as early as 30 min, but fewer than ~30% of BC surveyed had received these molecules. The rapidity with which anti-5′NT reached 100% of the BC surfaces (120 min) was particularly notable, in light of our earlier observation that anti-5′NT approached its steady-state distribution more slowly than APN (refer to Fig. 1 and text). Our interpretation is that internalization from the basolateral cell surface is the rate-limiting step in 5′NT transcytosis, rather than its long-distance transport step to the apical region or the final delivery to the apical surface. The delivery of HA4 to the subapical region and the apical PM lagged significantly behind the other apical PM proteins, and the label could not be detected in the membrane of all BC until 4 h. In contrast, pIgA-R reached the maximal fraction (~80%) of subapical regions as early as 30 min; but even at late chase times (after 4 h) only 50% of the microinjected BC contained detectable pIgA-R. This result is unlikely to be explained by cleavage of the receptor at the apical surface, since biochemical experiments have shown that generation of the 80-kD pIgA-R fragment is inefficient in WIF-B cells (our unpublished observation). However, use of an antibody to the receptor, rather than its physiological ligand (pIgA), might have caused this particular trafficking pattern, since the two ligands are known to exert different effects on pIgA-R transcytosis in MDCK cells (Mostov and Cardone, 1995).

Transcytosing Membrane Proteins Pass through the Same Subapical Compartment

We next performed cotrafficking experiments and confocal microscopic analysis to determine whether the different apically targeted proteins were distributed over the same intracellular compartments in the subapical area. We focused our analysis on early chase times (30 min), because the results of the microinjection experiments indi-

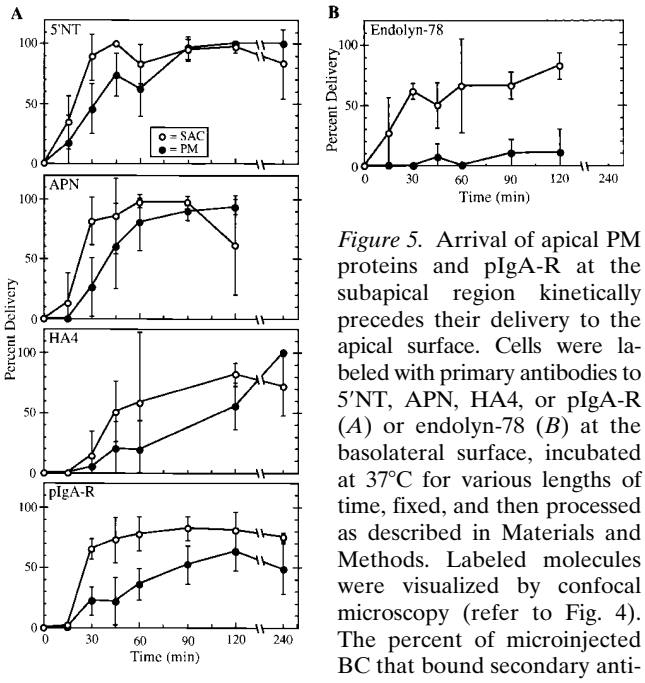

Figure 5. Arrival of apical PM proteins and pIgA-R at the subapical region kinetically precedes their delivery to the apical surface. Cells were labeled with primary antibodies to 5′NT, APN, HA4, or pIgA-R (*A*) or endolyn-78 (*B*) at the basolateral surface, incubated at 37°C for various lengths of time, fixed, and then processed as described in Materials and Methods. Labeled molecules were visualized by confocal microscopy (refer to Fig. 4). The percent of microinjected BC that bound secondary antibodies (●) and the percent of subapical regions containing label (○) were determined for each marker. Each point (mean ± SD) represents the results from between two and six different experiments with 44 ± 22 microinjected BC counted per time point (range of 16–89); the total numbers of microinjected BC counted were: 5′NT (*353*), APN (*401*), HA4 (*198*), pIgA-R (*550*), and endolyn-78 (*215*). Note in *B* that very few BC receive transcytosed endolyn-78, although the subapical region of most cells is positive as for apical PM proteins and the pIgA-R.

cated that, at this time, more cells contained positively labeled subapical compartments than they did positive BC. As shown in Fig. 6, the apical plasma membrane proteins APN and 5′NT (Fig. 6, *A* and *A′*) were clearly coincident in a subpopulation of small punctate structures seen throughout the cell and particularly in the area directly underneath the apical surface. Although light level microscopy cannot resolve membrane structures in close proximity, the similarity in the overall patterns of labeling suggests that both markers were present in the same transcytotic pathway. However, we also observed structures throughout the cells that were only positive for one or the other apical protein. Whether these variations reflect differences in the transport kinetics (refer to above) or the use of multiple endocytic–transcytotic pathways remains to be determined. Comparison of pIgA-R with 5′NT by confocal microscopy (Fig. 6, *B* and *B′*) confirmed that these two proteins also frequently coincided over the same subapical structures (i.e., those within ~1.5 μm of the apical surface) and some additional puncta deeper into the cells. These results suggested the existence of a common endomembrane system through which the multiple molecules pass on their way to the apical surface. We have termed the subapical compartment of this system SAC.

Conventional Endocytic Receptors Do Not Accumulate in SAC

To further explore the selectivity of basolateral-to-apical transcytosis of apical PM proteins, we examined the pathways taken by three endocytic receptors, the ASGP-R, Tf-R, and M6P-R, whose trafficking behaviors have been studied extensively in other cells. At steady state (Fig. 7, *A′* and *A′′*), ASGP-R was predominantly found in relatively large, irregularly shaped punctate structures close to the cell periphery, reminiscent of its localization in peripheral early endosomes of hepatocytes in situ. It was also found at the cell surface and in punctate or very fine tubulovesicular structures in the region between the nucleus and the BC close to the Golgi apparatus (data not shown). As a second and more ubiquitous early endosomal marker, we mapped the distribution of the Tf-R by internalization of fluorescently labeled Tf over a period of 30 min at 37°C. The steady-state distribution of Tf-R inferred from the localization of its ligand was very similar to that of ASGP-R in double-labeling experiments, i.e., it was seen mainly in peripheral punctate structures (Fig. 7, *B′* and *B′′*). Compared to ASGP-R, less Tf-R was found in the perinuclear region; however, when detectable, the label generally overlapped with ASGP-R–positive elements. A minor subpopulation of punctate structures containing both ASGP-R and Tf was found in the vicinity of the apical PM; these resembled basolateral peripheral endosomes in size and shape, hence we have called them early endosomes. M6P-R, often used as a late endosomal marker, was most abundant in the area between nucleus and BC, mainly concentrated in round punctate structures whose shapes and sizes were distinct from ASGP-R–containing elements in the same region (Fig. 7, *C′* and *C′′*). Thus, early and late endosomes are clearly identifiable in these cells.

The steady-state localization of each endocytic receptor provided a frame of reference for the further analysis of its dynamic distribution as it moved from the basolateral surface through the endocytic pathway. ASGP-R and M6P-R traffic was monitored using the same method as that used to track the movement of apical PM proteins. (The signal for Tf-Cy3 was too faint to follow after 4°C labeling and warming.) Antibodies to both receptors appeared to be delivered to the intracellular compartments corresponding to their steady-state locations (data not shown), and at no time did either antibody accumulate in the subapical region. This finding was confirmed by confocal microscopy in cotrafficking experiments where cells were simultaneously labeled with antibodies to 5′NT and ASGP-R (Fig. 6, *C–C′′*; see M6P-R further below). Although 5′NT antibodies were concentrated directly beneath the apical surface in a cap-like or patchy, ring-like pattern after 30 min of trafficking at 37°C (Fig. 6, *A′–C′*), ASGP-R was distributed over intracellular structures between the apical surface and the nucleus (Fig. 6, *C* and *C′′*) with no or little label in subapical structures. Both markers were sometimes colocalized in perinuclear structures (Fig. 6, *C–C′′*, *left BC*); however, in most cases, the 5′NT-positive structures in this region were quite distinct from those positive for ASGP-R (our unpublished observations).

Differences in the Trafficking of Lysosomal Membrane Proteins to Lysosomes

To complete our analysis of the trafficking behavior of molecules passing through the basolateral surface in WIF-B

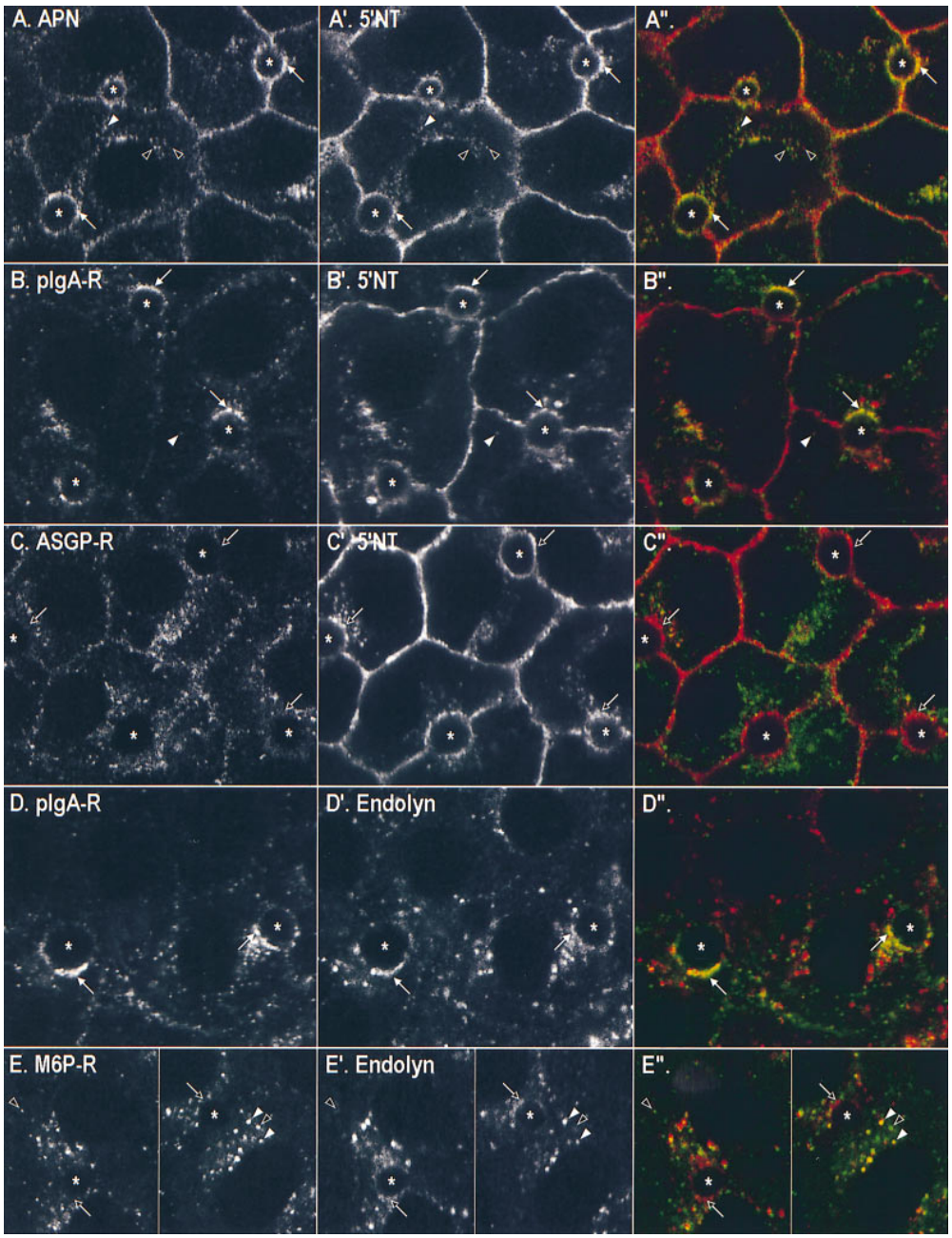

Figure 6. Cotrafficking of antibodies to various transcytotic and endocytic markers. Antibodies to two endogenous membrane antigens were bound simultaneously to the basolateral surface of living WIF-B cells at 0°C. The pairs were: (*A–A′′*) APN and 5′NT; (*B–B′*) pIgA-R and 5′NT; (*C–C′′*) ASGP-R and 5′NT; (*D–D′′*) pIgA-R and endolyn-78; or (*E–E′′*) M6P-R and endolyn-78. After unbound antibody was removed, the cells were incubated at 37°C for 30 min and then fixed and permeabilized. Primary antibodies were visualized by Cy5-conjugated (*A*, *B′*, *C*, *D′*, and *E′*) or FITC-conjugated secondary antibodies (*A′*, *B*, *C′*, *D*, and *E*). (*Right*) Merged images of the confocal fields are shown, with the images from the left column in *green* and images from the middle column in *red*. **, BC*; arrows in corresponding images mark the same location in the cell; *white arrows*, subapical structures containing both antibodies; and *black arrows*, structures containing one or no antibody. Arrowheads point to intracellular puncta containing both (*white*), one, or no (*black*) antibody.

cells, we followed antibodies to the lysosomal membrane proteins lgp120, lgp110, and endolyn-78. Although antibodies to all three proteins bound to the basolateral surface (in clustered patterns as for ASGP-R, M6P-R, and pIgA-R), only the antibody to endolyn-78 (mAb 501) gave a sufficiently strong signal after surface labeling at 0°C to be easily followed after warming to 37°C. Endolyn-78 is an extensively glycosylated membrane protein that, in unpolarized rat hepatoma cells and kidney fibroblasts, is found chiefly in lysosomes with lower levels in endosomal/prelysosomal structures (Croze et al., 1989). In WIF-B cells at steady state, endolyn-78 showed a very similar pattern. It was most highly concentrated in lgp120-positive structures, but had a somewhat broader distribution than this typical lysosomal marker, with some immunoreactivity found over various endosomes (Fig. 8, *A–A′′*). We also noted faint endolyn-78–positive rims around many BC. In trafficking experiments, antibody-tagged endolyn-78 approached a steady-state–like distribution within 120–180 min at 37°C, i.e., a predominantly lysosomal pattern with increasingly less label seen in an endosomal pattern. The colocalization with steady-state lgp120 (Fig. 8, *F–F′′*) at late time points was most prominent when leupeptin was included during trafficking, probably due to the inhibition of degradation of the anti–endolyn-78 mAb in lysosomes, as indicated by our measurements using ^{125}I-labeled antibody (Fig. 3 *B*). However, at earlier times (~30–60 min), we were surprised to see a striking concentration of trafficking endolyn-78 in subapical patches or rings around the BC (Fig. 6, *D′* and *E′* and Fig. 8, *C* and *D*). The rest of the label was in punctate structures that coincided often (but not always) with M6P-R, i.e., with late endosomes.

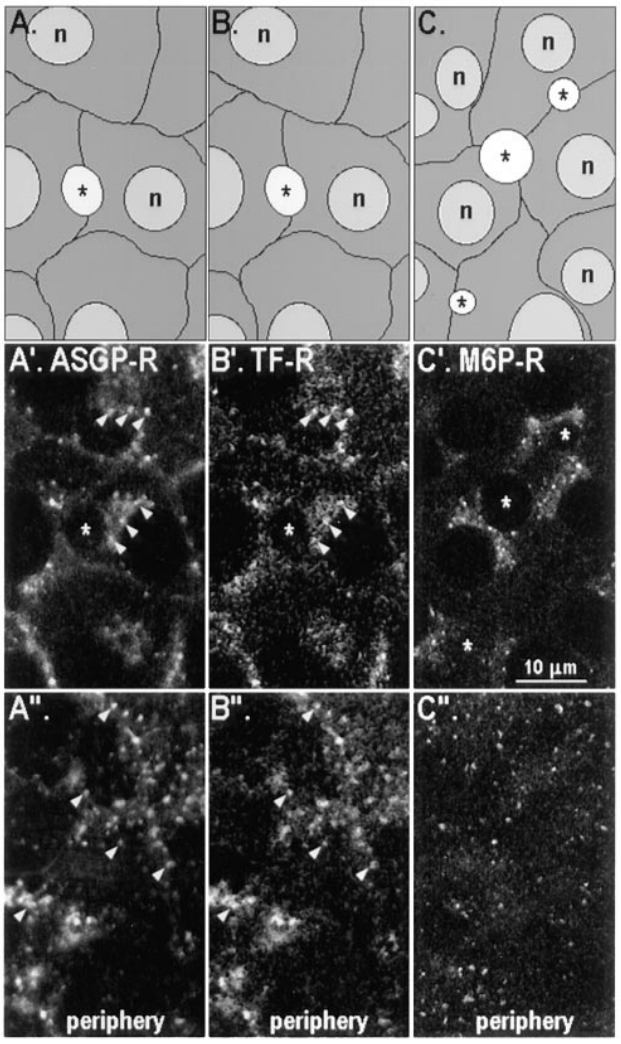

Figure 7. Three endocytic receptors are not concentrated in the subapical region of WIF-B cells at steady state. The distributions of ASGP-R (*A′* and *A′′*), Tf-R (*B′* and *B′′*), and M6P-R (*C′* and *C′′*) are shown at two locations in WIF-B cells: the confocal images in *A′*–*C′* were collected at the middle of cells and those in panels *A′′*–C′′ were collected close to the substratum. Schematic drawings of the cells in each field (*A*–*C*) are provided for orientation. Cells in (*A′* and *A′′*) and (*B′* and *B′′*) are identical cells that were first loaded with Cy3-conjugated Tf over 30 min at 37°C, and then fixed as described in Materials and Methods, and then subsequently incubated with pAb to ASGP-R. Cells in (*C′* and *C′′*) were fixed as usual and then incubated with pAb to M6P-R. Primary antibodies were detected by FITC-conjugated secondary antibodies. Note the colocalization of ASGP-R (*A′* and *A′′*) with Tf-R (*B′* and *B′′*) in the same structures, predominantly in peripheral endosomes (*arrowheads*). *, BC.

The M6P-R was never detected together with endolyn-78 in the ring-like structures (Fig. 6, *E*–*E′′*).

The transient concentration of endolyn-78 in elements adjacent to the BC was reminiscent of the subapical compartment through which apical PM proteins and the pIgA-R moved en route to the apical membrane. In fact, cotrafficking experiments with antibodies to endolyn-78 together with antibodies to APN (Fig. 8) or pIgA-R (Fig. 6, *D*–*D′′*) indicated that a subpopulation of the respective proteins colocalized in subapical structures at the light microscopic level. However, in comparison to our findings with two cotrafficked apical markers (Fig. 6, *A*–*A′′*), more puncta close to the BC were positive for only one or the other marker. This separation was especially evident for endolyn-78 and the pIgA-R (Fig. 6, *D*–*D′′*) and less so for endolyn-78 and APN (Fig. 8, *C*–*C′′* and *D*–*D′′*). The varying degrees of overlap may reflect the different final destinations of the proteins, since negligible amounts of endolyn-78 were transcytosed all the way to the apical surface, as determined two ways. First, in endolyn-78/APN cotrafficking experiments (Fig. 8), APN was found increasingly in brightly stained, relatively continuous rings at the BC, which appeared to be inside of the heteromorphous SAC, whereas endolyn-78 was not (Fig. 8, *C*–*C′′* and *D*–*D′′*). This qualitative impression was verified by microinjection experiments in which we quantified the arrival of endolyn-78 antibodies at the BC surface (Fig. 4 *B*). Such analysis revealed minimal delivery of endolyn-78 mAb to the apical membranes; only 11 of the 215 (i.e., 5%) microinjected BC scored positive over the entire time course of the trafficking experiments.

To address the question of whether the well-studied lysosomal marker lgp120 trafficked from the basolateral surface to lysosomes via SAC, it was necessary to increase the signal for lgp120 by incubating the cells at 37°C in the continuous presence of antibody (mAb GM10). Some label was seen in the prelysosomal/lysosomal area as early as 15 min and the signal increased over time without a dramatic change in the overall labeling pattern. Fig. 9, *A*–*A′′* shows the distribution of lgp120 antibodies after 30 min of uptake in a cotrafficking experiment with antibodies to APN, in comparison with endolyn-78 (mAb 501) labeled under the same conditions (Fig. 9, *B*–*B′′*). Endolyn-78 was distributed over the entire endocytic pathway, but was prominently seen in the subapical region where it showed a significant coincidence with APN (Fig. 9, *B*–*B′′*). In contrast, no overlap was detected between lgp120 and APN, although some lgp120-positive structures could be seen in the vicinity of the BC (Fig. 9, *A*–*A′′*).

EM Analysis Indicates That Endolyn-78 and APN Are in the Same Elements of SAC

To determine whether molecules going to two different locations (apical PM versus lysosomes) traversed the same SAC, we needed to visualize the trafficking antibodies in the EM under the conditions previously shown to label only or predominantly this compartment. Experiments using native antibody for trafficking followed by immunolocalization on ultrathin cryo-EM sections did not give a sufficiently high signal over background. Therefore, we prepared anti–endolyn-78 mAb and anti-APN pAb probes conjugated to HRP. HRP conjugates have been reported to faithfully mimic the intracellular route of the native protein (Wall et al., 1980; Hoppe et al., 1985; Hemery et al., 1996; Odorizzi et al., 1996); moreover, they yield a reaction product that can fill an entire compartment. In control experiments at the light level, we found that both IgG–HRP conjugates trafficked with similar kinetics and patterns as their unconjugated antibody. Furthermore, when both halves of the conjugate were visualized simultaneously (i.e., using anti-HRP and anti-IgG antibodies), the

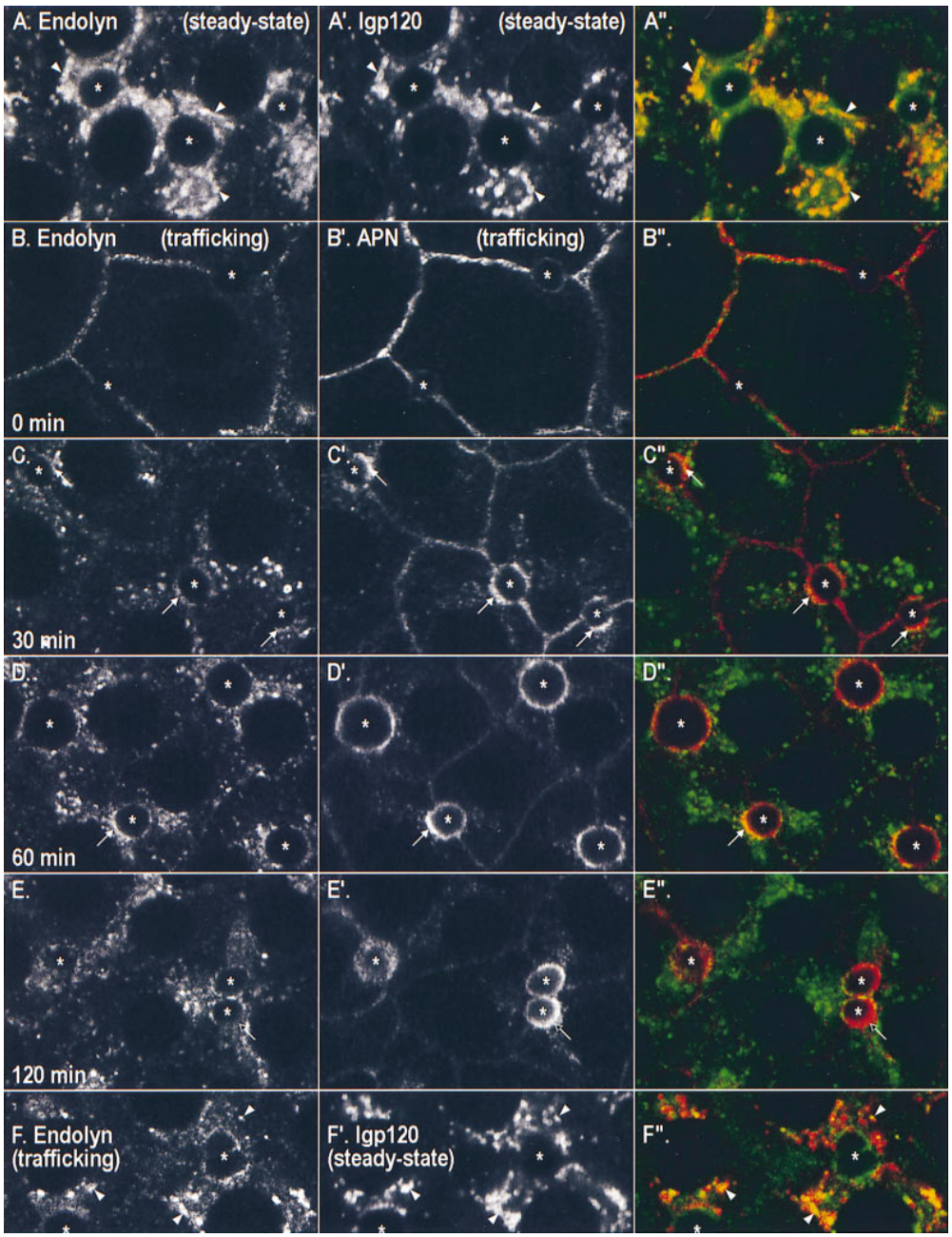

Figure 8. Endolyn-78 passes through a subapical compartment en route to lysosomes. The steady-state distributions of endolyn-78 and lgp120 revealed by double IMF are shown in (*A–A′′*). In (*B–B′′* to *E–E′′*) Antibodies to endolyn-78 (mAb 501, *left column*) and to APN (pAb, *middle column*) were bound simultaneously to the basolateral surface of living WIF-B cells at 0°C. The cells were then either fixed and permeabilized immediately (*B–B′′*) or warmed to 37°C for 30 min (*C–C′′*), 60 min (*D–D′′*), or 120 min (*E–E′′*) before fixation and permeabilization. In *F–F′′*, the living cells were labeled only with mAb501 (*F*) and then cells were colabeled after fixation with antibodies to lgp120 (*F′*). mAb 501 was visualized by FITC-conjugated secondary antibodies, the pAbs to lgp120, and APN by Cy5-conjugated secondary antibodies, respectively. (*Right column*) Merged images of corresponding pairs of confocal images are shown; the images from the left column are in *green* and images from the middle column are in *red.* *, BC; arrowheads and arrows point to areas of colocalizations of primary antibodies in lysosomes (*A–A′′* and *F–F′′*) and in SAC (*C–C′′* and *D–D′′*), respectively; *black arrows* (*E–E′′*), absence of endolyn-78 in APN-positive rings at later times.

overlap was essentially complete by IMF. This encouraged us to examine the trafficking behavior of these conjugates at the EM level under conditions where we would expect them to accumulate in SAC. Because the focus of the present study was the subapical region, we did not examine in detail the behavior of the probes elsewhere in the cell. Fig. 10 shows representative BC profiles in cells allowed to transport continuously present anti–APN–HRP (Fig. 10 *A*), anti–endolyn-78–HRP (Fig. 10 *B*), or unconjugated antibody (Fig. 10 *C*) for 30 min at 37°C. When the HRP conjugates were used, we saw tubulovesicular structures filled with HRP reaction product. The majority of unique positive structures were either cup-shaped or tubular/amorphous and <200 nm in size. Their prominent location underneath the BC surface and their tendency to form small clusters or patches are consistent with this class of HRP-positive structures being the SAC we identified by light microscopy. Several examples are presented at higher magnification in Fig. 10, *D* and *E*, which show clearly that APN and endolyn-78 are both present in the same types of structures. Quantification of the distribution of HRP reaction product in low-power images confirmed that labeled SAC elements predominated when either antibody was used (Fig. 11). Finally, similarly shaped structures were observed in untreated WIF-B cells and cells exposed to native IgG, suggesting that neither antibody trafficking nor the HRP induced their appearance (refer to Fig. 10 *C*).

SAC Consists of Unique Cup-shaped Structures and Tubular-Vesicular Elements

To obtain additional information on the ultrastructure of

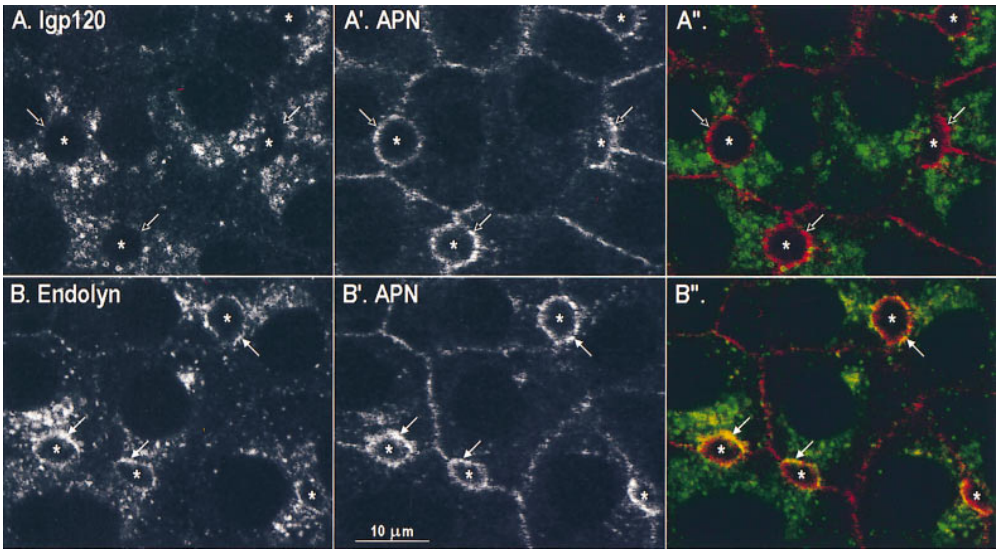

Figure 9. lgp120 does not traffic through the SAC. Antibodies to lgp120 (*A*; mAb GM10) or to endolyn-78 (*B*; mAb 501) were continuously internalized from the basolateral surface of WIF-B cells for 30 min at 37°C. Antibodies to APN were simultaneously internalized to provide a marker for SAC (*A′* and *B′*). The cells were then fixed and permeabilized, and the primary antibodies were detected using FITC-conjugated (*endolyn-78* and *lgp120*) or Cy5-conjugated (*APN*) secondary antibody. In *A″* and *B″*, the merged images of corresponding pairs of confocal images are shown; *left column*, *green*; *middle column*, *red.* *, BC; arrows in corresponding images mark the same location in the cell; *white arrows*, structures containing endolyn-78 antibody in SAC; *black arrows*, absence of corresponding lgp120 antibody.

SAC using an HRP-independent technique, we analyzed the trafficking behavior of gold-conjugated anti-5′NT mAb at the EM level. For these experiments, cells were incubated with antibody for 60 min at 37°C to increase the amount of internalized antigen–antibody complexes and make it possible to detect adequate numbers of gold particles in ultrathin sections (refer to Materials and Methods). The labeled cells were chased in medium without antibody for 3 h before fixation and processing for EM. Under these conditions, some aggregated gold particles were found in lysosomes (data not shown). This most likely represents a portion of gold-conjugated antibody mistargetted to lysosomes. However, about half of the gold particles were found at the apical surface or in subapical structures very similar to the ones observed with HRP-conjugated antibodies. This result is consistent with the gold particles corresponding to molecules trafficking along their physiological pathways, although perhaps more sluggishly. As seen in Fig. 12 *A*, gold particles were distributed along the lumenal face of the BC membrane, both on microvilli and flat regions, confirming that transcytosed 5′NT was indeed delivered to the apical PM. Sometimes, the gold was in

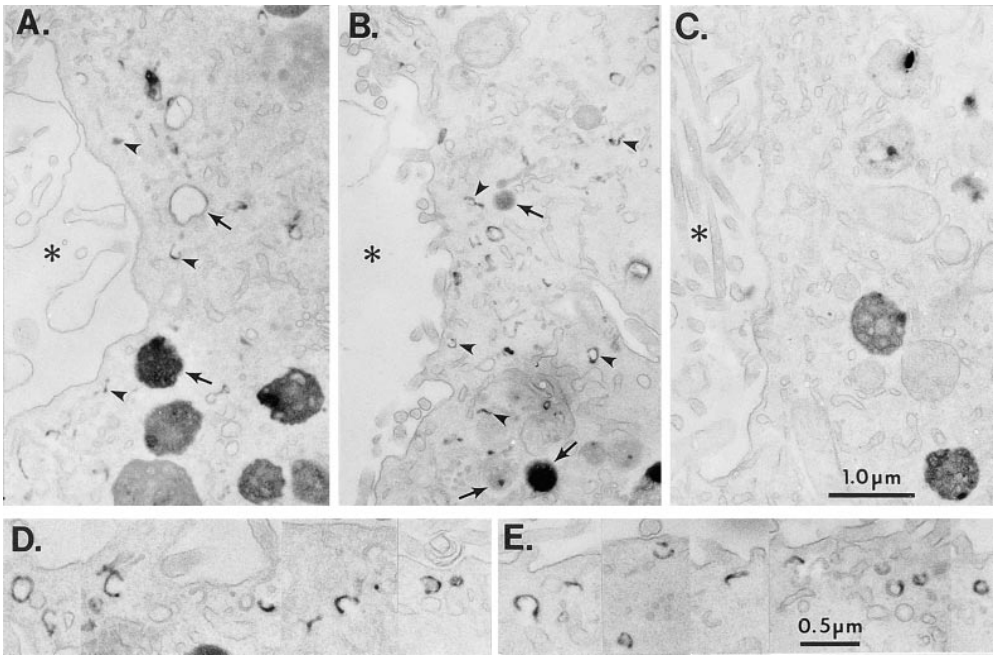

Figure 10. Anti–APN–HRP and anti–endolyn-78–HRP are both found in SAC in WIF-B cells. IgG–HRP conjugates (*A*, anti-APN; *B*, anti–endolyn-78) or IgG only (*C*, anti–endolyn-78; the other controls with anti-APN or no IgG looked identical) were applied to live cells as described in Materials and Methods. After 30 min of uptake at 37°C, cells were fixed and then processed for HRP cytochemistry. The resulting cell pellets were cut and then unstained sections were examined in the EM. In *A* and *B*, reaction product can be seen in cup-shaped and amorphous (*arrowheads*) structures located within 1.5 μm of the BC membrane. Similar structures are present but unlabeled in the controls (*C*). Reaction product can also be seen in larger circular and amorphous structures (*arrows*) under all conditions. Higher magnification views are presented of HRP-positive SAC structures in cells exposed to anti–APN–HRP (*D*) or anti–endolyn-78–HRP (*E*). *, BC.

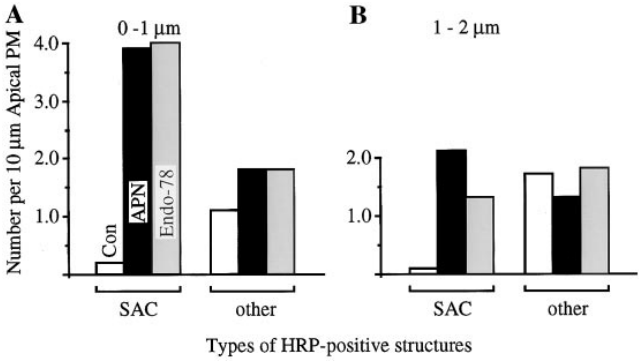

Figure 11. Distributions of HRP-positive structures in SAC after basolateral internalization of IgG–HRP conjugates. Cells were labeled with unconjugated IgG (*Con*), anti–APN–HRP (*APN*), or anti–endolyn-78–HRP (*Endolyn-78*) for 30 min, fixed, processed and then analyzed as described in Materials and Methods. HRP-positive structures in the subapical regions of photographed BC were classified by location (distance from the base of the nearest BC membrane) and shape (refer to examples in Fig. 10). The elements classified as SAC were small, amorphous (<200 nm) or cup-shaped structures completely filled with reaction product. The group *other* included structures (usually >200 nm in diam) containing patches of reaction product, as well as round structures (both small and large) and larger (>200 nm) amorphous structures, all filled with reaction product. Data from each experimental condition were pooled and presented as the average number of HRP-positive structures per 10-μm length of apical PM, at distances of 0–1 μm (*A*) and 1–2 μm (*B*) from the nearest BC. The total subapical areas analyzed (expressed as length of apical PM measured) and BC profiles counted, respectively, were: for the controls, 576 μm and 36 BC; for anti–APN–HRP, 414 μm and 20 BC; and for anti–endolyn-78–HRP, 352 μm and 24 BC.

small clusters along the BC membrane. The steady-state distribution of 5′NT along the apical surface (Fig. 12 *B*) was slightly more homogeneous than that of the trafficked antibody, and antigen was also detectable on the basolateral surface (data not shown). In contrast, virtually no antibody–gold probe was found at the basolateral cell surface or in basolateral regions of the cells under trafficking conditions (data not shown). To a significantly higher extent than at steady state, gold particles were present in subapical membranous structures (Fig. 12 *A*). Similar to HRP-labeled SAC structures, these elements were within ~1.5 μm of the BC membrane and were a mixture of tubules and vesicles (50–60-nm diam) and larger cup-shaped structures (158 nm ± 30 nm [n = 35]).

Discussion

In the present study, we have followed the itineraries of nine endogenous membrane proteins that have different steady-state distributions (apical PM, early endosomes, late endosomes, or lysosomes) but share the common property of passing through the basolateral PM at some point in their life cycle. Our approach was to use antibodies bound to the basolateral cohort of a particular membrane protein as reporters to follow the movement of these proteins. In all cases, the behavior of the antigen–antibody complexes was found to mirror the normal dynamics of the protein. Antibodies to several apical PM proteins (APN, DPPIV, HA4, and the GPI-anchored protein 5′NT) and to the pIgA-R were all selectively transcytosed from the basolateral to the apical membrane domains, supporting the hypothesis that, in WIF-B cells, newly synthesized molecules take an indirect route to the apical surface. Furthermore, the overall kinetics of apical PM protein delivery demonstrated that apical membrane traffic in WIF-B cells closely recapitulates that in liver. The apical PM proteins and pIgA-R passed through a SAC before delivery to the apical surface, as we had reported in vivo (Barr and Hubbard, 1993; Barr et al., 1995). Unexpectedly, the endosomal/lysosomal membrane protein endolyn-78 also appeared in SAC before reaching its final lysosomal destination. Such transient subapical accumulation was not seen for the lysosomal protein lgp120 or the endocytic receptors ASGP-R and M6P-R.

We propose that two endosomal sorting sites operate in the transcytotic pathway of WIF-B cells: (*a*) an early endosome located in the basolateral periphery that is analogous to early sorting endosomes in unpolarized cells, and (*b*) a subapical compartment located underneath the BC membrane that receives transcytosing PM proteins destined for the apical surface as well as a subset of other membrane proteins (e.g., endolyn-78) headed to other destinations (e.g., lysosomes). A schematic model of this view is presented in Fig. 13.

How Unique Is the Basolateral-to-Apical Transcytotic Pathway?

Although several models of transcytosis have been proposed, the precise mechanisms remain unknown. Current debate centers on whether the pathway includes steps (compartments) that are specific for proteins whose final destination is the apical PM. Although thinking in the field has been dominated by our knowledge of the behavior of the pIgA-R, it is important to keep in mind that the mechanisms for transcellular transport of other molecules may differ within the same epithelium and might even vary among epithelia. All models of basolateral-to-apical transcytosis in polarized epithelia begin with the steps of endocytosis from the basolateral PM and delivery to early sorting endosomes in the periphery of the cells. The very last step in the pathway, delivery to the apical PM, is likely mediated by some sort of transport vesicle. The minimal model of transcytosis (Schaerer et al., 1991) simply combined these events: transcytotic vesicles specifically enriched for apically directed proteins were proposed to bud directly from peripheral endosomes in the basolateral region, move across the cell, and then fuse with the apical PM. According to this view, the transcytotic vesicle and the transcellular movement would be specific for transcytosed molecules. It has become clear from work in MDCK cells (Apodaca et al., 1994; Barroso and Sztul, 1994; Odorizzi et al., 1996), Caco-2 cells (Knight et al., 1995), and hepatocytes (Hoppe et al., 1985; Barr and Hubbard, 1993; Barr et al., 1995; Hemery et al., 1996) that such a model is oversimplified. Transcytosed molecules pass through at least two different stations; early endosomes in the basolateral periphery, and a subapical endosome en route to the apical surface. The functional characteristics of this lat-

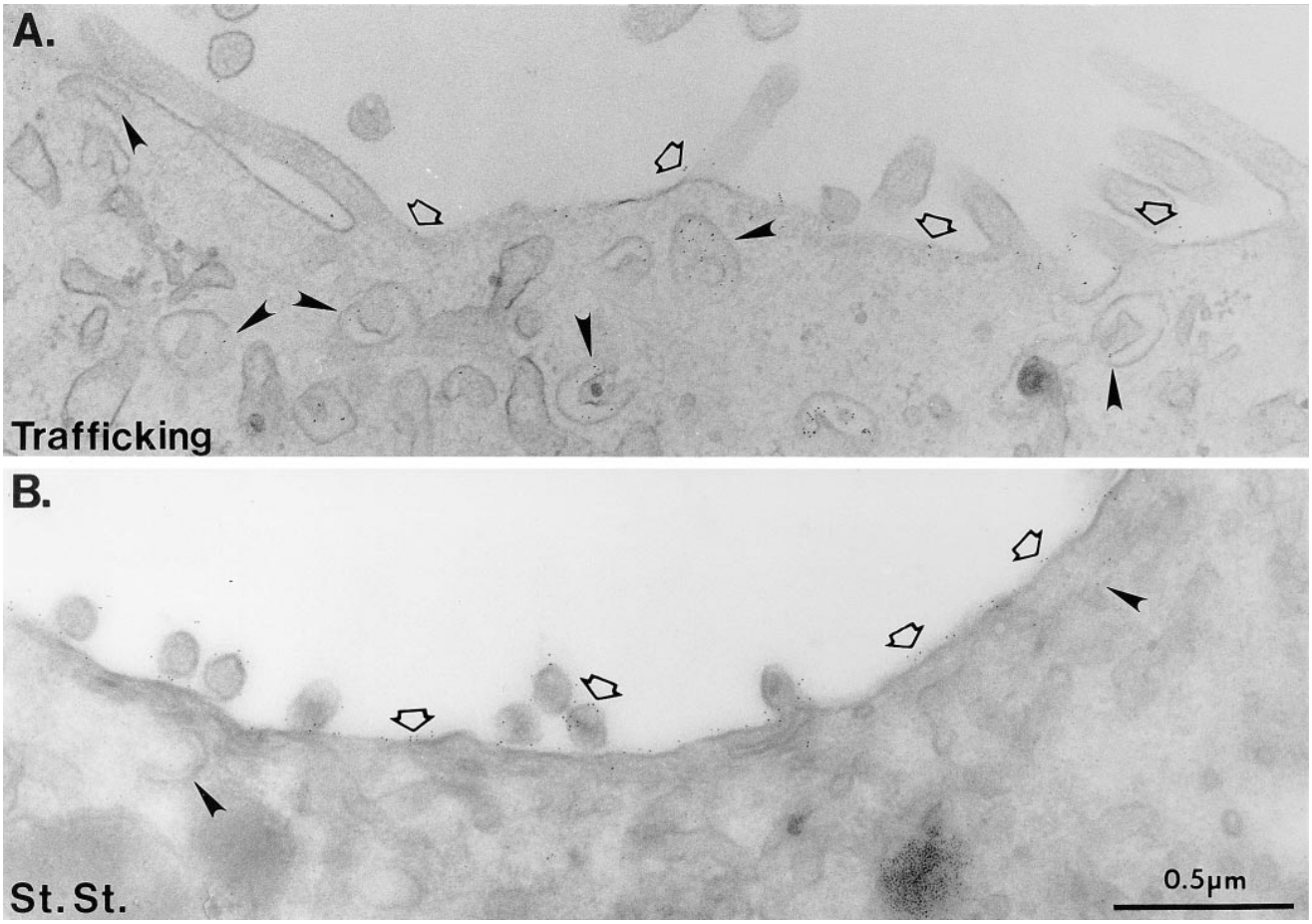

Figure 12. Transcytosed 5′NT antibody–gold complexes show a higher concentration in SAC than 5′NT at steady state. (*A*) Cells were labeled with anti-5′NT mAb conjugated to gold for 60 min at 37°C, rinsed, and then incubated for 3 h in the absence of antibody. Trafficked antibody–gold probe complexes were seen at the apical PM (*open arrows*). Just under the apical surface, label was observed in cup-shaped structures and small tubular-vesicular structures (*arrowheads*). (*B*) The steady-state EM level localization of 5′NT was determined on ultrathin cryosections. In addition to being present at the apical PM, steady-state 5′NT was occasionally localized to tubular-vesicular elements just under the apical surface (*right arrowhead*). *Left arrowhead*, cup-shaped structure.

ter membrane compartment are at issue and are a focus of the present study.

Recent work on pIgA-R transcytosis in MDCK cells has led to a model wherein transcytosis uses the endocytic membrane trafficking machinery present in all cells and does not require any unique transcytotic step (Apodaca et al., 1994). In this model, transcytotic cargo, together with basolaterally recycling receptors such as the Tf-R (a key feature of this model), is transported from the basolateral early endosome to an apical recycling compartment in the subapical cytoplasm. From here, molecules such as the pIgA-R are targeted for delivery to the apical membrane, possibly using the recycling leg of the apical endocytic pathway. Based on their studies of pIgA-R trafficking, again in MDCK cells, Barroso et al. (1994), have proposed a somewhat different model. As this group found little Tf-R in the apical region of the cell, they reasoned that the basolateral recycling endosome and apical recycling endosome (which also receives transcytotic proteins) are homologous but separate compartments. They concluded that specific carriers were necessary for transfer of transcytotic molecules to the apical region. Importantly, the last transfer step (from the subapical compartment to the surface) was found to be specific for transcytosed proteins, since it exhibited pharmacological characteristics distinct from the export of apically recycling proteins.

Our results support the hypothesis that, in hepatocytes, apical PM proteins use a transcytotic route that diverges early on from the major recycling pathways taken by the ASGP-R, Tf-R, or the M6P-R. Importantly, we found no recycling receptors in SAC at steady state or at any time during trafficking in vitro (this study), nor in hepatocytes in vivo as shown previously (Barr et al., 1995). Thus, in our view, it is highly unlikely that SAC acts as a major common sorting station for basolaterally internalized cargo in hepatocytes. Furthermore, the dynamic motile properties of kinetically early and late endocytic structures and SAC structures are quite distinct (Schroer et al., manuscript in preparation), again indicating a divergence into separate pathways of the two classes of internalized molecules (transcytotic versus recycling, refer to Fig. 13). On the other hand, all apical PM proteins and pIgA-R showed significant colocalization in SAC and other intracellular structures by confocal microscopy. Thus, these molecules

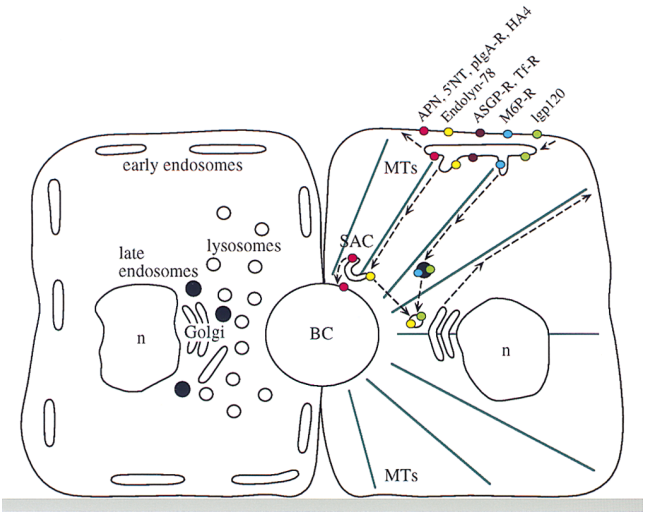

Figure 13. Summary of the steady-state organelle distributions and endogenous membrane protein trafficking patterns in WIF-B cells. (*Left*) The predominant locations of intracellular organelles are based on IMF analysis of the steady-state distributions of the following markers: ASGP-R, early/recycling endosomes; M6P-R, late endosomes; lgp120, lysosomes; mannosidase II and sialyltransferase, Golgi. (*Right*) The connections drawn between compartments in the endocytic–transcytotic pathway are based on results obtained in this study. Nearby peripheral (early) endosomes are the first intracellular station in which segregation of the major classes of basolaterally internalized membrane proteins occurs. Some molecules, as exemplified by the ASGP-R, M6P-R, and lgp 120, are recycled and/or delivered to compartments deeper in the cell where more recycling may occur. However, at least two classes of membrane proteins enter a third pathway; all apical PM proteins so far studied, including the pIgA-R, reach a SAC, as does at least one endosomal/lysosomal membrane protein, endolyn-78. Apical PM proteins and the pIgA-R are subsequently delivered to the apical surface, whereas the vast majority of endolyn-78 is not. At present we do not know whether endolyn-78 moves from SAC to lysosomes via late endosomes or uses a different (direct?) pathway.

appeared to use the same transcytotic pathway, regardless of their different protein structures (GPI-linked, transmembrane with short or long cytoplasmic tails). This finding agrees with earlier morphological (Barr and Hubbard, 1993) or subcellular fractionation studies (Quintart et al., 1989; Barr et al., 1995) in liver, in which DPPIV or 5′NT were found to codistribute with pIgA.

Hemery and co-workers (1996) have reported that transcytosis in polarized primary hepatocytes occurs in multiple intracellular transfer steps, which includes movement from peripheral endosomes to a juxtanuclear, pericentrosomal compartment, followed by delivery to tubulovesicular membranes in the subapical region. Both steps are microtubule dependent. In contrast, in polarized WIF-B cells, we observe only one transfer step, that leading to the transient accumulation of cargo in SAC. Perhaps the juxtanuclear compartment seen in primary hepatocytes is functionally equivalent to the SAC found in WIF-B cells, since both compartments serve as intermediates on the pathway to the apical surface and share a similar position with respect to cytoplasmic microtubules. The difference in the locations of the transcytosis intermediates may be a consequence of the fact that these two hepatic cells differ in the way their microtubules are organized: primary hepatocytes appear to contain a single, central microtubule organizing center whereas polarized WIF-B cells organize their microtubules preferentially about the apical surface (Ihrke et al., 1993; Meads and Schroer, 1995) in a pattern more similar to that of microtubules in liver (Martin, G., and A. Hubbard, manuscript in preparation) and other epithelia in vivo (Rizzolo and Joshi, 1993; Fath et al., 1994) and in culture (Bacallao et al., 1989; Meads and Schroer, 1995).

Features of the Hepatic Subapical Compartment

Our EM data indicate that SAC in WIF-B cells consists of two types of subapical endomembranes: tubulovesicular and cup-shaped structures. These are reminiscent of subapical structures in the livers of bile duct-ligated rats identified as part of the biogenetic pathway of newly synthesized apical membrane proteins (Barr and Hubbard, 1993; Barr et al., 1995). Tubulovesicular membrane elements are commonly found in regions of dynamic membrane sorting, such as the stations forming parts of the endosomal system and the *cis*- and *trans*-Golgi networks. We assume that local membrane fusion and budding events are involved in the delivery of transcytotic cargo to the cell surface, and that either SAC itself or vesicles derived from it are able to fuse with the apical PM. We speculate that the high surface:volume ratio afforded by the cup-shaped structures (which are a conspicuous feature in WIF-B cells) is favorable for delivering large amounts of membrane cargo and minimal amounts of fluid to the essentially closed BC in these cells.

The fact that SAC is on the endocytic pathway and is located in the apical region makes it by definition an apical endosome. However, the pattern of wortmannin-induced internalization of resident apical PM proteins suggests that SAC does not receive material from the apical surface (Tuma, P.L., and A.L. Hubbard, unpublished observations). Furthermore, our earlier morphological and biochemical results in vivo indicate that SAC does not contain recycling resident apical proteins (Barr and Hubbard, 1993; Barr et al., 1995). Thus, we propose that SAC is mainly a one-way sorting station to the apical PM and, for some molecules, to lysosomes (refer to our model in Fig. 13). Nonetheless, apical endocytosis must occur in polarized hepatic cells because estimates of the rate at which transcytotic vesicles (and thus, membrane surface area) are delivered to the BC (Crawford, 1996) are at least one order of magnitude greater than the rate at which apical membrane proteins and lipids are released into bile (Scott and Hubbard, 1992; Crawford et al., 1995). Moreover, apical endocytosis of 7-nitrobenz-2-oxal, 3-diazole (NBD)–sphingolipid analogues has been recently demonstrated in HepG2 cells (van Ijzendoorn et al., 1997). Early endosomes present in the apical region that receive cargo from the apical surface have been described in different epithelial cells, including MDCK (e.g., Bomsel et al., 1989; Apodaca et al., 1994; Barroso and Sztul, 1994) and Caco-2 cells (Hughson and Hopkins, 1990). The tubular aspects of these compartments are morphologically similar to SAC (50–60-nm tubules) (Parton et al., 1989; Apodaca et al., 1994; Knight et al., 1995; Odorizzi et al., 1996), although,

to our knowledge, no cup-shaped structures have been described. Since we cannot access the BC in living WIF-B cells without injuring them, there is currently no direct proof whether SAC and a (presumed) apically located recycling compartment are similar or distinct compartments, or alternatively, different subdomains of the same tubulovesicular endomembrane system.

Two Pathways Lead to Lysosomes

The different trafficking behaviors exhibited by the lysosomal membrane proteins followed in this study suggest the existence of two different pathways for delivery of proteins from the basolateral surface to lysosomes. The well-characterized lysosomal membrane glycoprotein, lgp120 (Hunziker and Geuze, 1996), appeared to move along the classic lysosomal pathway, i.e., from peripheral to late endosomes and then to lysosomes. The transient accumulation of endolyn-78 in a subapical compartment suggests that a significant fraction of this protein is diverted into the transcytotic pathway, presumably at the level of early endosomes. Our analysis of trafficking endolyn-78 at the ultrastructural level revealed the protein to be in subapical elements with cup-shaped or tubulovesicular morphology indistinguishable from APN- or 5′NT-containing transcytotic structures in the same location. In contrast to the apical PM proteins that were delivered to the BC, the bulk of the endolyn-78 molecules was subsequently routed to lysosomes. This implies that, if apical PM proteins and endolyn-78 molecules indeed enter the same SAC, sorting must occur here. We cannot completely rule out the possibility that endolyn-78 rapidly cycles through the PM and is directed from there to lysosomes; however, our microinjection experiments suggest that little endolyn-78 ever reaches the apical surface. Sequence analysis of endolyn-78 will hopefully reveal the potential targeting signals that determine this protein's circuitous itinerary.

Final Comments

Our comprehensive characterization of membrane protein dynamics in the polarized WIF-B cells allows us to draw a model of this cell's endocytic membrane trafficking pathways with some certainty (Fig. 13). We hypothesize that the subapical endomembranes containing transcytosed apical proteins are dynamic, that they are capable of sorting proteins to at least two different destinations (apical PM and lysosomes), and that they contain little, if any, cargo internalized from the apical surface. These intriguing results have raised new questions. For example, what fusion mechanism(s) are used to deliver cargo from SAC to the BC membrane? We have identified multiple plasma membrane target *N*-ethylmaleimide-sensitive factor attachment protein receptors in hepatocytes in vivo and WIF-B cells, at least three of which are present in the apical region/membrane (syntaxins 2, 3, and synaptosomal protein of 23 kD; Fujita et al., 1998; and unpublished data). Although syntaxin 3 has been found at the apical surface of other epithelial cells (for review see Delgrossi et al., 1997; Weimbs et al., 1997), syntaxin 2 reportedly has a more variable distribution (Low et al., 1996; Gaisano et al., 1996). Several small GTPases of the *rab* subfamily have been localized to the apical region in polarized epithelial cells (Ihrke and Hubbard, 1995; Goldenring et al., 1996; Calhoun and Goldenring, 1997; Novick and Zerial, 1997). Which rabs, if any, play a role in transcytosis and are any rabs uniquely associated with SAC? These and other questions remain to be answered in future studies.

We gratefully acknowledge W. Dunn, K. Himeno, J. Hutton, K. Kato, P. Luzio, R. Mains, I. Mellman, P. Nissley, K. Siddle, and Y. Tanaka for generously providing us with antibodies, and S. Mayor (Columbia University, New York) for Cy3-conjugated Tf and technical advice. We thank A. Kenworthy, M. Schell, and P. Tuma (all three from Johns Hopkins University and School of Medicine) for critical reading of the manuscript.

This work was supported by a National Institutes of Health grant (P01-NIDDK 44375).

Received for publication 13 March 1997 and in revised form 5 February 1998.

Note Added in Proof. A hepatic subapical membrane compartment that contains Annexin VI has been recently described (Ortega, D., A. Pol, M. Biermer, and S. Enrich. 1998. *J. Cell. Sci.* 111:261–269).

References

Anderson, R.G.W., M.S. Brown, U. Beisiegel, and J.L. Goldstein. 1982. Surface distribution and recycling of the low density lipoprotein receptor as visualized with antireceptor antibodies. *J. Cell Biol.* 93:523–531.

Apodaca, G., L.A. Katz, and K.E. Mostov. 1994. Receptor-mediated transcytosis of IgA in MDCK cells is via apical recycling endosomes. *J. Cell Biol.* 125: 67–86.

Bacallao, R., C. Antony, C. Dotti, E. Karsenti, E.H. Stelzer, and K. Simons. 1989. The subcellular organization of Madin-Darby canine kidney cells during the formation of a polarized epithelium. *J. Cell Biol.* 109:2817–2832.

Bailyes, E.M., M. Soos, P. Jackson, A.C. Newby, K. Siddle, and J.P. Luzio. 1984. The existence and properties of two dimers of rat liver ecto-5′-nucleotidase. *Biochem. J.* 221:369–377.

Barr, V.A., and A.L. Hubbard. 1993. Newly synthesized hepatocyte plasma membrane proteins are transported in transcytotic vesicles in the bile ductligated rat. *Gastroenterology.* 105:554–571.

Barr, V.A., L.J. Scott, and A.L. Hubbard. 1995. Immunoadsorption of hepatic vesicles carrying newly synthesized dipeptidyl peptidase IV and polymeric IgA receptor. *J. Biol. Chem.* 270:27834–27844.

Barroso, M., and E.S. Sztul. 1994. Basolateral to apical transcytosis in polarized cells is indirect and involves BFA and trimeric G protein-sensitive passage through the apical endosome. *J. Cell Biol.* 124:83–100.

Bartles, J.R., L.T. Braiterman, and A.L. Hubbard. 1985*a.* Endogenous and exogenous domain markers of the rat hepatocyte plasma membrane. *J. Cell Biol.* 100:1126–1138.

Bartles, J.R., L.T. Braiterman, and A.L. Hubbard. 1985*b.* Biochemical characterization of domain-specific glycoproteins of the rat hepatocyte plasma membrane. *J. Biol. Chem.* 260:12792–12802.

Bartles, J.R., H.M. Feracci, B. Stieger, and A.L. Hubbard. 1987. Biogenesis of the rat hepatocyte plasma membrane in vivo: comparison of the pathways taken by apical and basolateral proteins using subcellular fractionation. *J. Cell Biol.* 105:1241–1251.

Bomsel, M., K. Prydz, R.G. Parton, J. Gruenberg, and K. Simons. 1989. Endocytosis in filter-grown Madin-Darby canine kidney cells. *J. Cell Biol.* 109: 3243–3258.

Brändli, A.W., R.G. Parton, and K. Simons. 1990. Transcytosis in MDCK cells: identification of glycoproteins transported bidirectionally between both plasma membrane domains. *J. Cell Biol.* 111:2909–2921.

Burry, R.W. 1995. Pre-embedding Immunocytochemistry with Silver Enhanced Small Gold Particles. *In* Immunogold-Silver Staining: Principles, Methods, and Applications. M.A. Hayat, editor. CRC Press, Boca Raton, FL. 217–230.

Calhoun, B.C., and J.R. Goldenring. 1997. Two Rab proteins, vesicle-associated membrane protein 2 (VAMP-2) and secretory carrier membrane proteins (SCAMPs), are present on immunoisolated parietal cell tubulovesicles. *Biochem. J.* 325:559–564.

Cassio, D., C. Hamon-Benais, M. Guerin, and O. Lecoq. 1991. Hybrid cell lines constitute a potential reservoir of polarized cells: isolation and study of highly differentiated hepatoma-derived hybrid cells able to form functional bile canaliculi in vitro. *J. Cell Biol.* 115:1397–1408.

Coon, H.G., and M.C. Weiss. 1969. A quantitative comparison of formation of spontaneous and virus-produced viable hybrids. *Proc. Natl. Acad. Sci. USA.* 62:852–859.

Courtoy, P.J. 1993. Analytical subcellular fractionation of endosomal compartments in rat hepatocytes. *Subcell. Biochem.* 19:29–68.

Crawford, J.M. 1996. Role of vesicle-mediated transport pathways in hepatocellular bile secretion. *Sem. Liver Disease.* 16:169–189.

Crawford, J.M., G.M. Mockel, A.R. Crawford, S.J. Hagen, V.C. Hatch, S. Bar-

nes, J.J. Godleski, and M.C. Carey. 1995. Imaging biliary lipid secretion in the rat—ultrastructural evidence for vesiculation of the hepatocyte canalicular membrane. *J. Lipid Res.* 36:2147–2163.

Croze, E., I.E. Ivanov, G. Kreibich, M. Adesnik, D.D. Sabatini, and M.G. Rosenfeld. 1989. Endolyn-78, a membrane glycoprotein present in morphologically diverse components of the endosomal and lysosomal compartments: implications for lysosome biogenesis. *J. Cell Biol.* 108:1597–1613.

Delgrossi, M.H., L. Breuza, C. Mirre, P. Chavrier, and A. LeBivic. 1997. Human syntaxin 3 is localized apically in human intestinal cells. *J. Cell Sci.* 110: 2207–2214.

Drubin, D.G., and W.J. Nelson. 1996. Origins of cell polarity. *Cell.* 84:335–344.

Dunn, W.J. 1990. Studies on the mechanisms of autophagy: maturation of the autophagic vacuole. *J. Cell Biol.* 110:1935–1945.

Fath, K.R., G.M. Trimbur, and D.R. Burgess. 1994. Molecular motors are differentially distributed on Golgi membranes from polarized epithelial cells. *J. Cell Biol.* 126:661–675.

Fujita, H., P.L. Tuma, C.M. Finnegan, L.L. Locco, and A.L. Hubbard. 1998. Endogenous syntaxins 2, 3 and 4 exhibit distinct but overlapping patterns of expression at the hepatocyte plasma membrane. *Biochem. J.* 329:527–538.

Furuno, K., T. Ishikawa, K. Akasaki, S. Yano, Y. Tanaka, Y. Yamaguchi, H. Tsuji, M. Himeno, and K. Kato. 1989. Morphological localization of a major lysosomal membrane glycoprotein in the endocytic membrane system. *J. Biochem. (Tokyo).* 106:708–716.

Gaisano, H.Y., M. Ghai, P.N. Malkus, L. Sheu, A. Bouquillon, M.K. Bennet, and W.S. Trimble. 1996. Distinct cellular locations of the syntaxin family of proteins in rat pancreatic acinar cells. *Mol. Biol. Cell.* 7:2019–2027.

Geuze, H.J., J.W. Slot, G.J. Strous, J. Peppard, K. von Figura, A. Hasilik, and A.L. Schwartz. 1984. Intracellular receptor sorting during endocytosis: comparative immunoelectron microscopy of multiple receptors in rat liver. *Cell.* 37:195–204.

Goldenring, J.R., J. Smith, H.D. Vaughan, P. Cameron, W. Hawkins, and J. Navarre. 1996. Rab11 is an apically located small GTP-binding protein in epithelial tissues. *Am. J. Physiol.* 33:G515–525.

Greenwood, F.C., W.H. Hunter, and J.S. Glover. 1963. The preparation of ^{131}I-labeled human growth hormone of high specific radioactivity. *Biochem. J. (Tokyo).* 89:114–123.

Grimaldi, K.A., J.C. Hutton, and K. Siddle. 1987. Production and characterization of monoclonal antibodies to insulin secretory granule membranes. *Biochem. J. (Tokyo).* 245:557–566.

Gruenberg, J., and F.R. Maxfield. 1995. Membrane transport in the endocytic pathway. *Curr. Opin. Cell Biol.* 7:552–563.

Hammerton, R.W., K.A. Krzeminski, R.W. Mays, T.A. Ryan, D.A. Wollner, and W.J. Nelson. 1991. Mechanism for regulating cell surface distribution of Na^+,K(+)-ATPase in polarized epithelial cells. *Science.* 254:847–850.

Hayakawa, T., O.C. Ng, A. Ma, and J.L. Boyer. 1990. Taurocholate stimulates transcytotic vesicular pathways labeled by horseradish peroxidase in the isolated perfused rat liver (published erratum appears in *Gastroenterology* 99: 905). *Gastroenterology.* 99:216–228.

Hemery, I., A.-M. Durand-Schneider, G. Feldmann, J.-P. Vaerman, and M. Maurice. 1996. The transcytotic pathway of an apical plasma membrane protein (B10) in hepatocytes is similar to that of IgA and occurs via a tubular pericentriolar compartment. *J. Cell Sci.* 109:1215–1227.

Hopkins, C.R., A. Gibson, M. Shipman, and K. Miller. 1990. Movement of internalized ligand-receptor complexes along a continuous endosomal reticulum. *Nature.* 346:335–339.

Hoppe, C.A., T.P. Connolly, and A.L. Hubbard. 1985. Transcellular transport of polymeric IgA in the rat hepatocyte: biochemical and morphological characterization of the transport pathway. *J. Cell Biol.* 101:2113–2123.

Hubbard, A.L., and Z.A. Cohn. 1972. The enzymatic iodination of the red cell membrane. *J. Cell Biol.* 55:390–405.

Hubbard, A.L., J.R. Bartles, and L.T. Braiterman. 1985. Identification of rat hepatocyte plasma membrane proteins using monoclonal antibodies. *J. Cell Biol.* 100:1115–1125.

Hughson, E.J., and C.R. Hopkins. 1990. Endocytic pathways in polarized Caco-2 cells: identification of an endosomal compartment accessible from both apical and basolateral surfaces. *J. Cell Biol.* 110:337–348.

Hunziker, W., and H.W. Geuze. 1996. Intracellular trafficking of lysosmal membrane proteins. *Bioessays.* 18:379–389.

Ihrke, G., and A.L. Hubbard. 1995. Control of Vesicle Traffic in Hepatocytes. *In* Progress in Liver Diseases. J.L. Boyer and R.K. Ockner, editors. W.B. Saunders, Philadelphia, PA. 63–99.

Ihrke, G., E.B. Neufeld, T. Meads, M.R. Shanks, D. Cassio, M. Laurent, T.A. Schroer, R.E. Pagano, and A.L. Hubbard. 1993. WIF-B cells: an in vitro model for studies of hepatocyte polarity. *J. Cell Biol.* 123:1761–1775.

Kiess, W., J.F. Haskell, L. Lee, L.A. Greenstein, B.E. Miller, A.L. Aarons, M.M. Rechler, and S.P. Nissley. 1987. An antibody that blocks insulin-like growth factor (IGF) binding to the type II IGF receptor is neither an agonist nor an inhibitor of IGF-stimulated biologic responses in L6 myoblasts. *J. Biol. Chem.* 262:12745–12751.

Knight, A., E. Hughson, C.R. Hopkins, and D.F. Cutler. 1995. Membrane protein trafficking through the common apical endosome compartment of polarized Caco-2 cells. *Mol. Biol. Cell.* 6:597–610.

Ladinsky, M.S., and K.E. Howell. 1992. The *trans*-Golgi network can be dissected structurally and functionally from the cisternae of the Golgi complex by brefeldin A. *Eur. J. Cell Biol.* 59:92–105.

Leunissen, J.L.M., and J.R. De Mey. 1989. Preparation of Gold Probes. *In* Immuno-gold Labeling in Cell Biology. A.J. Verkleij and J.L.M. Leunissen, editors. CRC Press, Boca Raton, FL. 3–16.

Lewis, V., S.A. Green, M. Marsh, P. Vihko, A. Helenius, and I. Mellman. 1985. Glycoproteins of the lysosomal membrane. *J. Cell Biol.* 100:1839–1847.

Lippincott-Schwartz, J., and D.M. Fambrough. 1986. Lysosomal membrane dynamics: structure and interorganellar movement of a major lysosomal membrane glycoprotein. *J. Cell Biol.* 102:1593–1605.

Lisanti, M.P., and E. Rodriguez-Boulan. 1990. Glycophospholipid membrane anchoring provides clues to the mechanism of protein sorting in polarized epithelial cells. *Trends Biochem. Sci.* 15:113–118.

Low, S.-H., T. Chapin, L.G. Weimbs, M.K. Kömüves, M.K. Bennett, and K.E. Mostov. 1996. Differential localization of syntaxin isoforms in polarized Madin-Darby canine kidney cells. *Mol. Biol. Cell.* 7:2007–2018.

Marsh, E.W., P.L. Leopold, N.L. Jones, and F.R. Maxfield. 1995. Oligomerized transferrin receptors are selectively retained by a lumenal sorting signal in a long-lived endocytic recycling compartment. *J. Cell Biol.* 129:1509–1522.

Matter, K., and I. Mellman. 1994. Mechanisms of cell polarity: sorting and transport in epithelial cells. *Curr. Opin. Cell Biol.* 6:545–554.

Maurice, M., M.J. Schell, B. Lardeux, and A.L. Hubbard. 1994. Biosynthesis and intracellular transport of a bile canalicular plasma membrane protein: studies in vivo and in the perfused rat liver. *Hepatology.* 19:648–655.

Mays, R.W., K.A. Siemers, B.A. Fritz, A.W. Lowe, G. van Meer, and W.J. Nelson. 1995. Hierarchy of mechanisms involved in generating Na/K-ATPase polarity in MDCK epithelial cells. *J. Cell Biol.* 130:1105–1115.

Meads, T., and T.A. Schroer. 1995. Polarity and nucleation of microtubules in polarized epithelial cells. *Cell Motil. Cytoskeleton.* 32:273–288.

Mellman, I., and H. Plutner. 1984. Internalization and degradation of macrophage Fc receptors bound to polyvalent immune complexes. *J. Cell Biol.* 98: 1170–1177.

Mevel-Ninio, M., and M.C. Weiss. 1981. Immunofluorescence analysis of the time-course of extinction, reexpression, and activation of albumin production in rat hepatoma-mouse fibroblast heterokaryons and hybrids. *J. Cell Biol.* 90:339–350.

Milgram, S.L., E.Y. Chang, and R.E. Mains. 1996. Processing and routing of a membrane-anchored form of proneuropeptide Y. *Mol. Endocrin.* 10:837–846.

Mostov, K.E., and M.H. Cardone. 1995. Regulation of protein traffic in polarized epithelial cells. *Bioessays.* 17:129–138.

Musil, L.S., and J.U. Baenziger. 1988. Proteolytic processing of rat liver membrane secretory component. Cleavage activity is localized to bile canalicular membranes. *J. Biol. Chem.* 263:15799–15808.

Novick, P., and M. Zerial. 1997. The diversity of Rab proteins in vesicle transport. *Curr. Opin. Cell Biol.* 9:496–504.

Odorizzi, G., A. Pearse, D. Domingo, I.S. Trowbridge, and C.R. Hopkins. 1996. Apical and basolateral endosomes of MDCK cells are interconnected and contain a polarized sorting mechanism. *J. Cell Biol.* 135:139–152.

Parton, R.G., K. Prydz, M. Bomsel, K. Simons, and G. Griffiths. 1989. Meeting of the apical and basolateral endocytic pathways of the Madin-Darby canine kidney cell in late endosomes. *J. Cell Biol.* 109:3259–3272.

Porter, R.R. 1959. The hydrolysis of rabbit gamma-globulin and antibodies with crystalline papain. *Biochem. J. (Tokyo).* 73:119–225.

Quintart, J., P. Baudhuin, and P.J. Courtoy. 1989. Marker enzymes in rat liver vesicles involved in transcellular transport. *Eur J. Biochem.* 184:567–574.

Reaves, J.R., N.A. Bright, B.M. Mullock, and J.P. Luzio. 1996. The effect of wortmannin on the localisation of lysosomal type I integral membrane glycoproteins suggests a role for phosphoinositide 3-kinase activity in regulating membrane traffic late in the endocytic pathway. *J. Cell Sci.* 109:749–762.

Rizzolo, L.J., and H.C. Joshi. 1993. Apical orientation of the microtubule organizing center and associated g-tubulin during polarization of the retinal pigment epithelium in vivo. *Dev. Biol.* 157:147–156.

Rodriguez-Boulan, E., and S.K. Powell. 1992. Polarity of epithelial and neuronal cells. *Annu. Rev. Cell Biol.* 8:395–427.

Rodriguez-Boulan, E., and C. Zurzolo. 1993. Polarity signals in epithelial cells. *J. Cell Sci.* 17(Suppl.):9–12.

Roth, J., D. Taatjes, J. Lucocq, J. Weinstein, and J. Paulson. 1985. Demonstration of an extensive trans-tubular network continuous with the Golgi-apparatus stack that may function in glycosylation. *Cell.* 43:287–295.

Sandoval, I.V., and O. Bakke. 1994. Targeting of membrane proteins to endosomes and lysosomes. *Trends Cell Biol.* 4:292–297.

Schaerer, E., M.R. Neutra, and J.P. Kraehenbuhl. 1991. Molecular and cellular mechanisms involved in transepithelial transport. *J. Membr. Biol.* 123:93–103.

Schell, M.J., M. Maurice, B. Stieger, and A.L. Hubbard. 1992. 5′nucleotidase is sorted to the apical domain of hepatocytes via an indirect route (published erratum appears in *J. Cell Biol.* 123:767). *J. Cell Biol.* 119:1173–1182.

Scott, L.J., and A.L. Hubbard. 1992. Dynamics of four rat liver plasma membrane proteins and polymeric IgA receptor. Rates of synthesis and selective loss into the bile (published erratum appears in *J. Biol. Chem.* 268:19160). *J. Biol. Chem.* 267:6099–6106.

Shanks, M.R., D. Cassio, O. Lecoq, and A.L. Hubbard. 1994. An improved polarized rat hepatoma hybrid cell line. Generation and comparison with its hepatoma relatives and hepatocytes in vivo. *J. Cell Sci.* 107:813–825.

Simons, K., and S.D. Fuller. 1985. Cell surface polarity in epithelia. *Annu. Rev. Cell Biol.* 1:243–288.

Simons, K., P. Dupree, K. Fiedler, L.A. Huber, T. Kobayashi, T. Kurzchalia, V. Olkkonen, S. Pimplikar, R. Parton, and C. Dotti. 1992. Biogenesis of Cell-

Surface Polarity in Epithelial Cells and Neurons. *In* Cold Spring Harb. Symp. Quant. Biol. 57:611–618.
Slot, J.W., and H.J. Geuze. 1984. Gold Markers for Single and Double Immunolabeling of Ultrathin Cryosections. *In* Immunolabeling for Electronmicroscopy. J.M. Polak and I.M. Varndell, editors. Elsevier Science, New York. 129–142.
Slot, J.W., and H.J. Geuze. 1985. A new method for preparing gold probes for multiple labeling cytochemistry. *Eur. J. Cell Biol.* 38:87–93.
Tokuyasu, K.T. 1989. Use of poly(vinylpyrrolidone) and poly(vinyl alcohol) for cryoultramicrotomy. *Histochem. J.* 21:163–171.
van Deurs, B., S.H. Hansen, O.W. Petersen, E.L. Melby, and K. Sandvig. 1990. Endocytosis, intracellular transport and transcytosis of the toxic protein ricin by a polarized epithelium. *Eur. J. Cell Biol.* 51:96–109.
van Genderen, I., and G. van Meer. 1995. Differential targeting of glucosylceramide and galactosylceramide analogues after synthesis but not during transcytosis in Madin-Darby canine kidney cells. *J. Cell Biol.* 131:645–654.
van Ijzendoorn, S.C.D., M.M.P. Zegers, J.W. Kok, and D. Hoekstra. 1997. Segregation of glucosylceramide and sphingomyelin occurs in the apical to basolateral transcytotic route in HepG2 cells. *J. Cell Biol.* 137:347–357.
Venkatachalan, M.A., and H.D. Fahimi. 1969. The use of beef liver catalase as a protein tracer for electron microscopy. *J. Cell Biol.* 42:480–489.
Vogel, L.K., O. Noren, and H. Sjostrom. 1995. Transcytosis of aminopeptidase-N in Caco-2 cells is mediated by a non-cytoplasmic signal. *J. Biol. Chem.* 270: 22933–22938.
Vogel, L.K., M. Spiess, H. Sjostrom, and O. Noren. 1992. Evidence for an apical sorting signal on the ectodomain of human aminopeptidase N. *J. Biol. Chem.* 267:2794–2797.
von Figura, K., V. Gieselmann, and A. Hasilik. 1984. Antibody to mannose 6-phosphate receptor induces receptor deficiency in human fibroblasts. *EMBO (Eur. Mol. Biol. Organ.) J.* 3:1281–1286.
Wall, D.A., G. Wilson, and A.L. Hubbard. 1980. The galactose-specific recognition system of mammalian liver: the route of ligand internalization in rat hepatocytes. *Cell.* 21:79–93.
Weimbs, T., S.H. Low, S.J. Chapin, and K.E. Mostov. 1997. Apical targeting in polarized epithelial cells: there's more afloat than rafts. *Trends Cell Biol.* 7:393–399.
Weissman, A.M., R.D. Klausner, R. Krishnamurty, and J.B. Harford. 1986. Exposure of K562 cells to anti-receptor monoclonal antibody OKT9 results in rapid redistribution and enhanced degradation of the transferrin receptor. *J. Cell Biol.* 102:951–958.
Weisz, O.A., C.E. Machamer, and A.L. Hubbard. 1992. Rat liver dipeptidylpeptidase IV contains competing apical and basolateral targeting information. *J. Biol. Chem.* 267:22282–22288.
Wollner, D.A., and W.J. Nelson. 1992. Establishing and maintaining epithelial cell polarity. Roles of protein sorting, delivery and retention. *J. Cell Sci.* 102: 185–190.
Yamashiro, D.J., B. Tycko, S.R. Fluss, and F.R. Maxfield. 1984. Segregation of transferrin to a mildly acidic (pH 6.5) para-Golgi compartment in the recycling pathway. *Cell.* 37:789–800.
Zaal, K.J., J.W. Kok, R. Sormunen, S. Eskelinen, and D. Hoekstra. 1994. Intracellular sites involved in the biogenesis of bile canaliculi in hepatic cells. *Eur. J. Cell Biol.* 63:10–19.
Zhu, D., and B.U. Pauli. 1991. Generation of monoclonal antibodies directed against organ-specific endothelial cell surface determinants. *J. Histochem. Cytochem.* 39:1137–1142.